https://doi.org/10.5194/egusphere-2025-5795
Preprint. Discussion started: 19 February 2026

70 Years of Glacier Loss on the Nevados de Chillán volcanic complex, Chile

Millie Spencer[1], Emma Tyrrell[1], Robert Clasing[2], Alfonso Fernandez[3], Enrique Muñoz[2,4], Pablo A. Mendoza[5,6], and Noah P. Molotch[1]

[1]Department of Geography, Institute of Arctic and Alpine Research, University of Colorado, Boulder, 80309, USA
[2]Department of Civil Engineering, Universidad Católica de la Santísima Concepción, Concepción, 4090340, Chile
[3]Department of Geography, Universidad de Concepción, Concepción, 4070386, Chile
[4]Centro de Investigación en Biodiversidad y Ambientes Sustentables CIBAS, Concepción, 4090340, Chile
[5]Department of Civil Engineering, Universidad de Chile, Santiago, 8370449, Chile
[6]Advanced Mining Technology Center (AMTC), Universidad de Chile, Santiago, 8370449, Chile

Correspondence to: Millie Spencer (millie.spencer@colorado.edu)

Abstract. Glaciers on the Nevados de Chillán volcanic complex are rapidly retreating, with anticipated consequences for agroforestry, tourism, and regional human and ecological security. Quantifying their mass balance is critical for understanding current meltwater contributions and for anticipating future water availability as these glaciers continue to shrink. Here we estimate the geodetic mass balance of all 28 documented glaciers on the Nevados de Chillán complex. An uncrewed aerial vehicle (UAV) campaign conducted in March 2024 provided updated elevation data for 11 glaciers on the complex, allowing calculation of volume change from 1954–2024 (70 years). For the remaining 17 glaciers, we analyzed airplane and satellite digital elevation models (DEMs) to estimate volume change from 1954–2000 (46 years). Our results show a clear acceleration in glacier mass loss after 2000 for the glaciers surveyed with UAV data. Mean annual specific mass balance of the Cerro Blanco subcomplex accelerated from -0.41 ± 0.33 m w.e. y^{-1} (1954-2024) to -0.60 ± 0.29 m w.e. y^{-1} (2000-2024), while that of the Las Termas subcomplex increased from -0.13 ± 0.32 m w.e. y^{-1} (1954-2024) to -0.36 ± 0.18 m w.e. y^{-1} (2000-2024). Regional water resource planning should consider how increasing glacier melt rates on the Nevados de Chillán complex will impact the timing and volume of future water availability.

1 Introduction

Mountain glaciers have immense value due to their support of municipal and agricultural water demands, alpine ecosystems, and mountain tourism (Immerzeel et al., 2020). As global temperatures rise, mountain glaciers are retreating on average

https://doi.org/10.5194/egusphere-2025-5795
Preprint. Discussion started: 19 February 2026

(Hugonnet et al., 2021; Van Tricht et al., 2025; Zemp et al., 2015). Quantifying this retreat is essential to forecasting downstream water availability (Aguayo et al., 2024; Mark et al., 2015; Ultee et al., 2022).

Glacier retreat is well studied in Chile, particularly in the Maipo basin surrounding the capital city of Santiago, and on the Patagonian Ice Fields (e.g. Ayala et al., 2020; Carrasco-Escaff et al., 2023; Farías-Barahona et al., 2020; Schaefer et al., 2015). Compared to the extensive literature on glaciers in central Chile and Patagonia, south-central Chile remains relatively understudied, leaving the current state of its glaciers not yet fully characterized. Although several important studies have documented glacier retreat in this region (e.g. Barria et al., 2018; Brock et al., 2007; Rivera et al., 2006), further research is needed to quantify glacier loss rates and improve water availability forecasting as glaciers continue to shrink.

Glacier melt's relative contributions are becoming increasingly important as south-central Chile's traditionally humid environment shifts from year-round precipitation to increasingly rain-free summer seasons, steadily decreasing annual mean precipitation and increased drought frequency and severity (Garreaud et al., 2020; Rubio-Álvarez and McPhee, 2010). Even small glaciers have been shown to have significant impacts on basin runoff (Nolin et al., 2010; Clark et al., 2015), suggesting that small alpine glaciers in south-central Chile, such as those on the Nevados de Chillán, may have outsized impacts on downstream water availability.

Nevados de Chillán is a glaciated volcanic complex in the Ñuble region of south-central Chile that houses a ski resort and hot spring by the same name and is a major tourist destination for the region. Existing geodetic studies of Nevados de Chillán's glaciers solely assess change in glacier area and do not document change in glacier volume (e.g. Zenteno et al., 2004). While glacier area change provides some insight into climate impacts, precise glacier elevation change measurements are required to accurately reconstruct the volume of meltwater contributed by mountain glaciers in south central-Chile (e.g. Mejías et al., 2025). Our study provides such data for Nevados de Chillán.

Despite frequent eruption events, the Nevados de Chillán volcanic complex was last estimated as having 28 mountain glaciers (Fig. 1B) (DGA, 2022) (Fig. 1B). However, it is not clear how many of these glaciers no longer exist or are now debris covered. Published observations of the glaciers of Nevados de Chillán indicate a >45% reduction in area from 1863-1975, and >90% loss in glacier area by 2019 (Philippi, 1863; DGA, 2022). While previous studies documented change in glacier area, there are no long-term estimates of glacier mass balance that account for all glaciers in the complex. Despite changes in glacier area providing insights into glacier retreat, robust mass-balance measurements are necessary to accurately determine volume change, sensitivity to climate changes, relative contribution of glacier melt to regional water availability, mountain hazards,

https://doi.org/10.5194/egusphere-2025-5795
Preprint. Discussion started: 19 February 2026

and other dynamics that control high-elevation landscapes (Owen et al., 2009). Many of these issues remain unexplored in Ñuble.

Previous studies have provided estimates of Chilean glacier mass balance at a variety of scales, ranging from regional to specific glacier analyses. Dussaillant et al. (2019) reported a mass balance of -0.31 ± 0.19 m w.e. yr^{-1} in the Central Andes and -0.57 ± 0.22 m w.e. yr^{-1} in Northern Patagonia. Caro et al. (2024) estimated a 2000-2019 mean annual mass balance of -0.29 ± 0.14 m w.e. yr^{-1} for the Maipo River basin (33°S), versus -0.47 ± 0.19 m w.e. yr^{-1} for the Baker River basin (47°S). On the Echarren Norte Glacier (33°S), Farías-Barahona et al. (2019) estimated a mean glacier mass balance of −0.68 ± 0.09 m w.e. yr^{-1} from 1955-2015, showing a sharp increase in glacier loss from 2010 onwards with a mass balance of −1.20 ± 0.09 m w.e. yr^{-1}.

While glacier area change analyses and regional-scale assessments provide useful benchmarks, variability in specific glacier mass balance underscores the importance of finer-scale studies rather than relying solely on regional averages or nearby glacier measurements. Therefore, this paper provides geodetic mass balance estimates for the period 1954-2000 (n=46 years) for all glaciers on Nevados de Chillán, and for 2000-2024 (n=24 years) for the 11 glaciers inventoried in our UAV campaign. Further, we analyze geographic and temporal patterns in glacier melt rates, crucial to inform landscape changes and impacts on regional water management.

2 Study Area

The Nevados de Chillán (36.86°S, 71.39°W) volcanic complex is in the Ñuble Region of south-central Chile (Fig. 1A). The volcanic complex spans approximately 14 kilometers from northwest to southeast and comprises 13 stratovolcanoes, which are divided into the Cerro Blanco subcomplex and Las Termas subcomplex (Fig. 1B) (Dixon et al., 1999; Naranjo et al., 2008). The maximum altitude of the study area is on the summit of the Cerro Blanco complex, 3151 meters above sea-level [m a.s.l]. The glaciers vary in size and are found on all aspects of the peaks. The largest glacier on the complex, Glaciar Nevado, is housed on the Cerro Blanco subcomplex, has a south-westerly aspect, and covered approximately 0.68 km^2 in 2019 (Fig. 1C) (DGA, 2022). The Chilean Water Directorate (*Dirección General de Aguas*, DGA) estimates that there are 28 glaciers on the complex. Despite several glaciers in the saddle between the Cerro Blanco and Las Termas subcomplex and on the north face of the Las Termas subcomplex disappearing, remaining glaciers fractured into multiple ice bodies (DGA, 2014; 2022). From 2000 to 2019, glacier area decreased from 2.90 x 10^6 m^2 to 1.21 x 10^6 m^2, amounting to a 58.3% decrease in glacier area (DGA, 2014; 2022). Melt from Nevados de Chillán's glaciers has immeasurable value, supporting ecological diversity and downstream water availability. The Nevados de Chillán complex falls within the Itata River basin, which spans an area of 11,294 km^2 (Bobadilla et al., 2024).

https://doi.org/10.5194/egusphere-2025-5795
Preprint. Discussion started: 19 February 2026

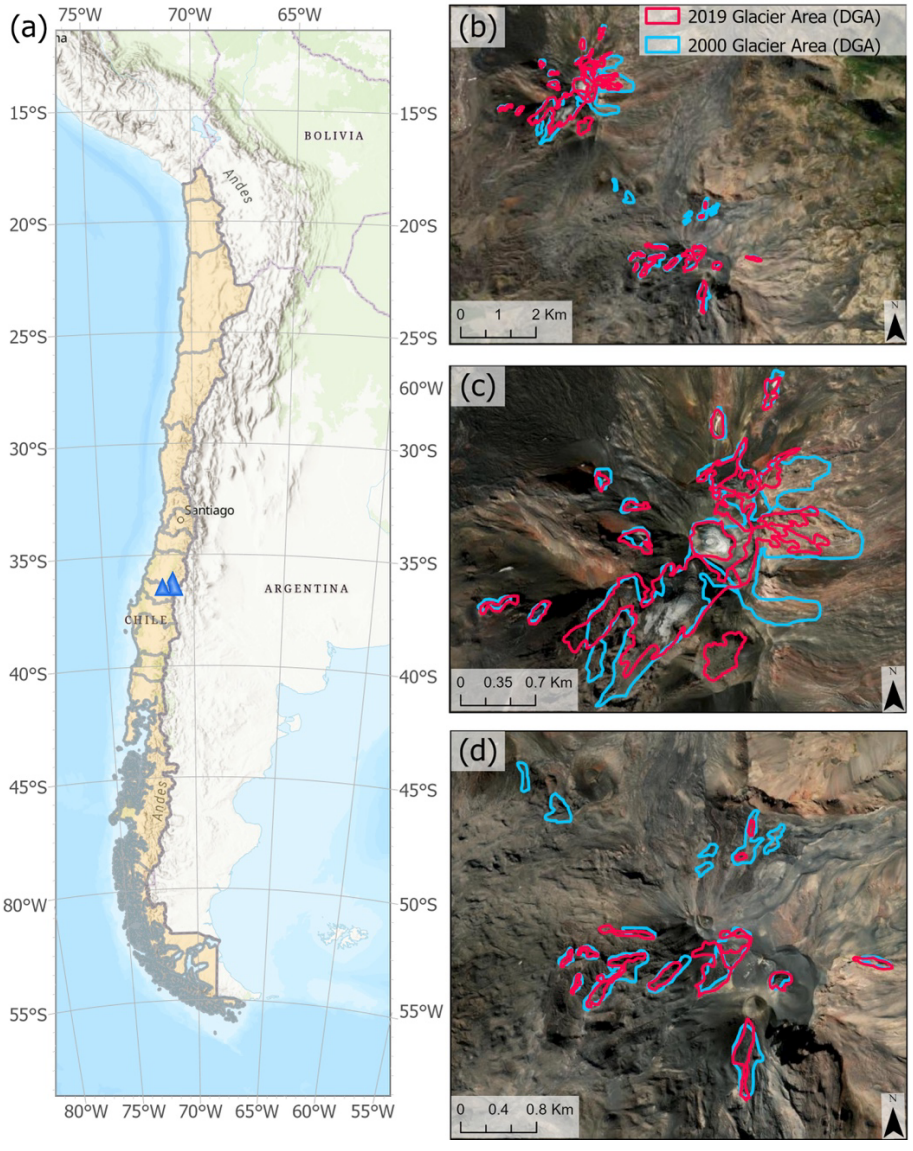

Figure 1: A) Study area in the Ñuble region of Chile, B) satellite view (Maxar Technologies © 2025) of the Cerro Blanco and Las Termas subcomplexes on the Nevados de Chillán volcanic complex with year 2000 and 2019 glacier areas (DGA, 2014; 2022) shown in cyan and magenta, respectively, C) zoomed in on the Cerro Blanco subcomplex and D) the Las Termas subcomplex.

The region has a Mediterranean climate, characterized by warm, dry summers and wet winters with heavy precipitation (Bobadilla et al., 2024). Given the near total absence of precipitation in summer months, glaciers and seasonal snowmelt are essential components of summer streamflow in the Ñuble region (Ayala et al., 2016; Ragettli and Pellicciotti, 2012). Notably, agriculture accounts for 96.3% of water consumption in the Itata River basin, with irrigation demand peaking in late summer when glacier runoff is highest (Bobadilla et al., 2024; Webb et al., 2021; Bellisario et al., 2013; McCarthy et al., 2022). As

https://doi.org/10.5194/egusphere-2025-5795
Preprint. Discussion started: 19 February 2026

droughts become more frequent, and Ñuble's environment shifts from year-round precipitation to increasingly rain-free summer seasons, summer glacier discharge plays an increasingly critical role in meeting water needs (Bobadilla et al., 2024; Ayala et al., 2016; Ragettli and Pellicciotti, 2012; Garreaud et al., 2020; Rubio-Álvarez and McPhee, 2010).

3 Methods

Figure 2 presents the methodological workflow for implementing a geodetic mass balance approach, a highly reliable method to estimate glacier mass loss (Huss and Hock, 2015; Hugonnet et al., 2021; Cogley, 2009; Schuster et al., 2023). A georeferenced aerial image (*Instituto Geográfico Militar*, IGM) from 1954 and Shuttle Radar Topography Mission (SRTM) image from 2000 are used to reconstruct historic glacier surface elevations. However, given the scarcity of open-source global DEMs available for recent years, the work herein relies on the production of uncrewed aerial vehicle (UAV)-derived DEMs to provide glacier elevation measurements after 2000. We conducted a UAV field campaign in March 2024 to generate a detailed DEM of the complex (Sect. 3.1 and 3.2). We differenced historic aerial (IGM) and satellite (SRTM) DEMs from the 2024 UAV DEM and clipped to the glacier areas reported by the DGA for the years 2000 and 2019 (DGA 2014; 2022) to generate glacier volume loss and calculate mean annual geodetic mass balance (Sect. 3.4). Finally, we discuss the implications of these findings for glacier resilience and future water resources availability (Sect. 4 and 5).

https://doi.org/10.5194/egusphere-2025-5795
Preprint. Discussion started: 19 February 2026

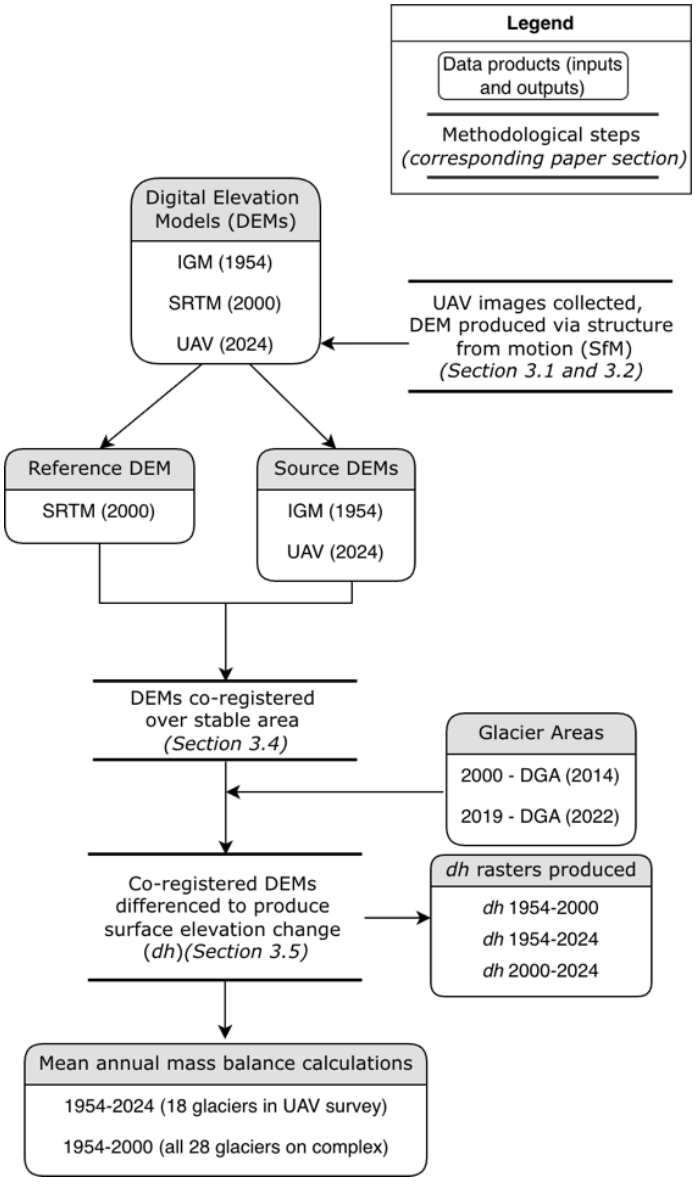

Figure 2: Methodological workflow detailing the DEMs accessed (DGA and SRTM) and created (UAV) to represent glacier elevation (Sections 3.1 and 3.2), DEM co-registration (Section 3.3) and differencing to estimate glacier mass balance (Section 3.4).

3.1 UAV Image Acquisition

The DJI Mavic 3 Enterprise (M3E) UAV integrated with a GPS Real-Time Kinematic (RTK) solution module was used for RGB imaging of Nevados de Chillán and the generation of a DEM. The DJI M3E UAV houses a L2D-20c Hasselblad brand camera designed for photogrammetry. This camera has 4/3-inch Complementary Metal Oxide Semiconductor (CMOS) digital image sensor, 20 MP effective resolution, and mechanical shutter. We utilized GPS-RTK for cm accuracy positioning during

https://doi.org/10.5194/egusphere-2025-5795
Preprint. Discussion started: 19 February 2026

flight and for precise georeferencing of captured pictures. GPS-RTK provides a solution to improved UAV positioning in lieu of ground control points (Wigmore and Mark, 2017). RTK position accuracy is 1 cm + 1 ppm (horizontal) and 1.5 cm + 1 ppm (vertical).

The UAV flight campaign was carried out during the best light conditions, around midday on the 12 and 14 March 2024 and in peak-ablation season (i.e. snow-free conditions). Automated flight plans were designed using the DJI Pilot application, with a fixed flight altitude of 145 m above ground level for the Cerro Blanco subcomplex, and 315 m above ground level for the Las Termas subcomplex. Higher flight altitude was required for the Las Termas subcomplex to map the larger area (11.5 km^2 compared to 1.75 km^2 for the Cerro Blanco subcomplex) with limited battery capacity, which yielded higher resolution images of Cerro Blanco compared to Las Termas (Sect. 3.2). The flight path was programmed with 70% and 80% horizontal and vertical overlap respectively, to ensure successful 3-D model construction through SfM in image post-processing. Due to heavy winds and technical difficulties, manual flight and image capture was required over many sections on the Cerro Blanco subcomplex, resulting in a greater root mean square error (RMSE) when compared to the Las Termas subcomplex.

3.2 UAV Image Processing

AgiSoft Metashape (Version 2.1.2) software, widely used in similar glacier UAV studies, was used to process the UAV images (e.g. Wigmore and Mark, 2017; Kaufmann et al., 2021; Bisset et al., 2022; Wigmore and Molotch, 2023; Rossini et al., 2023). As in previous studies, images were processed using the SfM photogrammetry workflow in Metashape, a proprietary software by AgiSoft (Westoby et al., 2012; Over et al., 2021). Metashape SfM reconstructed the 3-D geometry of the study scene by identifying common points that occur in multiple images from different angles and distances (Westoby et al., 2012). These common points were tracked from image to image, enabling estimation of camera position and object coordinates which were continuously refined using non-linear least-squares minimization as additional images are processed (Westoby et al., 2012). A dense point cloud was generated by aligning these tie-points with a multiple-view stereo algorithm (Frazier and Singh, 2021; Kaufmann et al., 2021). Next, a triangular irregular network mesh was used to estimate 3-D point positions within the selected coordinate system to create a continuous mesh (Westoby et al., 2012). This mesh was then smoothed and an orthomosaic was produced. Finally, a digital elevation model (DEM) was generated from the dense point cloud (Frazier and Singh, 2021; Rossini et al., 2023).

The relatively lower flight altitudes over Cerro Blanco yielded a higher DEM resolution in this area (7.82 cm/pixel) compared to Las Termas (16.70 cm/pixel). However, the RMSE was larger for the Cerro Blanco subcomplex than the Las Termas subcomplex (20.03 versus 9.24 cm, respectively), which was likely a result of manual UAV flying and image capture on the Cerro Blanco subcomplex.

https://doi.org/10.5194/egusphere-2025-5795
Preprint. Discussion started: 19 February 2026

3.3 Satellite and Airborne Elevation Products and Methods

To compute glacier volume loss over time, we compared our 2024 UAV-derived DEM to two historic DEMs: one built from topographic maps produced by the IGM and the 2000 SRTM DEM product. To increase the accuracy of our analysis, all DEMs used were from the southern hemisphere ablation season (February-March) to minimize the presence of snow cover influencing ground elevation measurements.

Table 1: Sources for DEMs differenced for glacier volume loss estimates

Source	Vehicle Type	Sensor Type	Survey Date	Resolution [per pixel]
IGM	Airplane	Aerial photo	1954	30 m
SRTM	Satellite	C-band radar	2000	30 m
This study	UAV	4/3" CMOS RGB Camera	2024	7.82 cm (Cerro Blanco) and 16.70 cm (Las Termas)

3.3.1 Instituto Geográfico Militar (IGM) DEM

The IGM DEM product was generated from interpolating elevations from the 1:50,000 scale topographic map "Nevados de Chillán" produced by the IGM. Published in 1968 using aerial photos from 1954, this map was built using UTM Zone 19 South and provides contour lines every 25 m and spot heights of several summits across the study area, referred to the PSAD56 datum. As the map exists only in paper format, the copy available in the Geography Department at the Universidad de Concepción was scanned, georeferenced, and digitized using the methods described in DGA (2022). The map was then displayed on ArcGIS Pro for georeferencing, employing coordinates of more than a dozen locations corresponding to the intersections between lines defining the UTM coordinate grid closest to the glacier. Subsequently, contour lines and spot heights were digitized on screen, producing one shapefile of polylines (contours) and points (spot heights) with their corresponding elevation assigned as an attribute. Next, the polylines were disaggregated into their respective vertex points and merged with the point shapefile, a merged file that was then reprojected into WGS84 datum. These points were used to create a 30 m resolution DEM via interpolation employing the Inverse Distance Weighting (IDW) method.

3.3.2 Shuttle Radar Topography Mission (SRTM) DEM

The second DEM used in this study was the SRTM 1 Arc-Second Global DEM for February 2000 (USGS, 2018). SRTM provides a global 30 m resolution DEM produced from a C-band (5.6 cm) radar antenna with observations from 11-22 February 2000, during peak summer ablation for Chilean glaciers, making it an excellent reference for glacier ice elevation (USGS, 2018).

Both Hugonnet et al. (2021) and Dussaillant et al. (2020) utilized the DEM co-registration and differencing approach used herein to estimate mean glacier elevation change. However, Hugonnet et al. (2021) and Dussaillant et al. (2020) use Advanced Spaceborne Thermal Emission and Reflection Radiometer (ASTER) (optical stereo images) where we use SRTM (radar

https://doi.org/10.5194/egusphere-2025-5795
Preprint. Discussion started: 19 February 2026

interferometry) (USGS, 2018). The different methods used to produce ASTER and SRTM images has implications for DEM accuracy – when compared to SRTM, ASTER suffers from signal attenuation and vertical accuracy error over steep slopes and snow and ice. Moreover, SRTM resolves elevation by comparing two images taken seconds apart, whereas ASTER represents a composite elevation from ~2000-2004, which risks incorporation of winter scenes and thus distorting glacier elevation with seasonal snow cover. For these reasons, we chose SRTM over ASTER to represent the year ~2000 glacier elevation.

3.4 DEM reprojection, alignment, and co-registration

All three DEMs were first reprojected to the same coordinate system and resolution, and the UAV DEMs are reprojected to a 30 m resolution to match the IGM and SRTM DEMs. All DEMs are aligned on the same grid as the SRTM DEM with ESRI's *arcpy* package (v.2.3.0) using bilinear interpolation.

Next, we co-registered the reprojected and aligned DEMs over stable terrain surrounding the glaciers. DEM co-registration improves accuracy when comparing elevation between DEMs by reducing horizontal and vertical shifts between images (Berthier et al., 2024). As in Shean et al. (2023) and Berthier et al. (2024), we implemented the Nuth and Kääb (2011) algorithm, which was packaged by Shean et al. (2016) in an open-source Python workflow (See: Appendix A-C). We co-registered the IGM (1954) DEM to the SRTM DEM masking out all glaciers on the Nevados de Chillán complex using the year 2000 glacier polygons provided by DGA (2014) and co-registering the DEMs over surrounding stable terrain. We co-registered the Cerro Blanco and Las Termas complexes separately because the DEMs have different spatial resolutions, and thus co-registration to the SRTM DEM yielded different error values. Maps of stable areas used for glacier co-registration, along with error calculations, are provided in Appendix A-C.

3.5 Computing Glacier Mass Balance

Glacier mass balance was computed by clipping the co-registered DEMs to the 2000 and 2019 glacier areas provided by DGA (2014, 2022) and differencing the co-registered DEMs to calculate the change in height per pixel (Δh). Vertical ice loss was then converted to specific mean annual glacier mass balance, via the relative average densities of glacier ice (ρ_{ice}) and water (ρ_{water}), measured in meters water equivalent per unit area per year (m w.e. yr^{-1}):

$$Mass - Balance = \sum_{i=1}^{n} \Delta h_i \frac{\rho_{ice}}{\rho_{water}} n^{-1}\,, \quad (1)$$

Where ρ_{ice} = 850 kg m^{-3}, ρ_{water} = 1,000 kg m^{-3}, n is the number of years between DEM dates, and Δh is the change in glacier elevation per pixel, i, within the glacier area for the year 2000 (DGA, 2014) or 2019 (DGA, 2022).

This workflow was repeated for each glacier on the complex. Due to weather and logistical limitations of our field work, only 11 of the 28 inventoried glaciers on Nevados de Chillán were covered by the UAV DEM, consisting of the southwestern face

https://doi.org/10.5194/egusphere-2025-5795
Preprint. Discussion started: 19 February 2026

of Cerro Blanco, and the western and southern faces of the Las Termas subcomplex. As a result, cumulative mean annual mass balance was calculated for all 28 glaciers between 1954-2000, whereas mass balance was only calculated for 11 glaciers after the year 2000.

Mass-balance uncertainty was calculated as time-averaged normalized mean absolute deviation (NMAD), a method for identifying outliers in non-normally distributed data, which was calculated in the co-registration process over stable areas as:

$$NMAD = 1.4826 \cdot median(|\Delta z_i - m_{\Delta z}|)\,, \quad (2)$$

Where Δz_i = (z_{GCPi} - z_{DEMi}) are errors and $|\Delta z_i|$ are absolute errors, calculated from control points computed for each DEM before and after co-registration (Shean et al., 2016). NMAD is commonly used to represent elevation measurement error because DEM errors rarely display normal distributions, making RMSE and standard deviations less accurate due to their assumptions of normal distribution (Hugonnet et al., 2021; Shean et al., 2016). NMAD was then converted to m w.e. for comparison with our mass balance estimates (Appendix A-C). NMAD values were calculated for the Las Termas UAV DEM (NMAD = 5.12 m w.e.), Cerro Blanco UAV DEM (NMAD = 8.14 m w.e.), and IGM DEM (NMAD = 25.14 m w.e.), through their co-registration with the SRTM DEM. The larger NMAD values of the IGM and Cerro Blanco UAV DEMs was likely a result of larger data variability, outliers, and/or irregular data distribution. Moreover, we found a correlation between the size of the stable areas surrounding glaciers and the NMAD—more stable areas were measured over the Las Termas subcomplex than over Cerro Blanco, corresponding to lower NMAD values over the former than the latter. To produce mean annual mass-balance error estimates, NMAD was divided by the number of years between DEM observations, *n,* (e.g. SRTM(2000) - IGM(1954) = 46 years).

3.6 Hydroclimate Data

Precipitation data were sourced from two meteorological stations nearest the Nevados de Chillán complex—Las Trancas and Diguillín—located approximately 10 and 18 km aerial distance and 1366 m and 1899 m below the complex, respectively. Maximum and minimum monthly temperature data were obtained from the DGA's Diguillín meteorological station via CR2 (https://explorador.cr2.cl/), while no temperature data was available for the Las Trancas station. Daily streamflow data were also provided for the Diguillín station. Monthly precipitation and streamflow data were summed to compute cumulative annual precipitation for the Las Trancas and Diguillín meteorological stations. Daily minimum and maximum temperature data were averaged to derive mean daily temperature. From these, three temperature time series were generated representing minimum, mean, and maximum values.

Temperature, precipitation, and streamflow were analyzed for the full record and for summer months (December–February; DJF). Hydroclimatic trends were quantified using Sen's slope estimator (Sen, 1968), which is robust to outliers, missing values, and non-normal distributions that commonly characterize climatic and hydrological time series. Sen's slope computes the median of all pairwise slopes between observations,

https://doi.org/10.5194/egusphere-2025-5795
Preprint. Discussion started: 19 February 2026

$$\hat{\beta} = median\left(\frac{x_j - x_i}{j - i}\right), for\ j > i, \quad (3)$$

yielding a distribution-free estimate of the monotonic trend magnitude. Trends were evaluated over the full record and separately for pre- and post-2000 periods to enable comparison with glacier mass balance changes. Statistical significance of trends was assessed using the nonparametric Mann–Kendall test (Mann, 1954; Kendall, 1948), following Burkey (2021) via the *pymannkendall* package in Python. Significance was evaluated at the 95% level ($p < 0.05$).

To identify potential hydroclimatic regime shifts, we applied the E-Divisive multiple change-point algorithm implemented in the *ecp* package in R (James and Matteson, 2015). This method is fully nonparametric and detects changes in the underlying distribution of a time-ordered sequence of multivariate observations; in this case, vectors of temperature, precipitation, streamflow station measurements (Matteson and James, 2014). Rather than assuming changes in only the mean or variance, the method assesses whether two adjacent segments of the time series differ in their joint distribution using a divergence measure based on U-statistics (Matteson and James, 2014). Candidate change points are chosen to maximize this divergence, and statistical significance is evaluated using permutation testing. A minimum window size of 10 years was imposed on both sides of a candidate change point to reduce sensitivity to short-term variability and to ensure that shifts represent sustained hydroclimatic changes relevant to regime analysis.

4 Results

4.1 DEM co-registration and error calculation

By co-registering the UAV DEMs and IGM DEM to the SRTM DEM, we reduce geolocation errors and thus improve the accuracy of our elevation change and mass balance calculations (Shean et al., 2023). Pre- and post-co-registration median (50^{th} percentile) signed error and NMAD were calculated for each DEM. In all three cases, co-registering the DEMs with the SRTM DEM reduced the median positive vertical error. When co-registering the Cerro Blanco UAV DEM to the SRTM DEM, positive vertical error surrounding Glacier Nevado was reduced from a median value of 19.88 m to 0.13 m, whereas NMAD stayed the same. For the Las Termas UAV DEM, co-registration reduced positive vertical error from a median value of 27.51 m to 0.03 m. NMAD reduced from 5.68 m to 5.12m . Finally, the positive vertical error on the IGM DEM reduced from a median of 17.78 m to 6.52 m, and a NMAD of 31.62 m to 25.64 m with co-registration.

4.2 Glacier elevation change

Across both the Cerro Blanco and Las Termas subcomplexes, and all three analysis periods (1954-2000, 2000-2024, and 1954-2024), glaciers thinned on average (Fig. 3). For the Las Termas subcomplex, mean thinning increased when using the 2019 glacier polygons versus the 2000 glacier polygons, whereas the opposite was true for the Cerro Blanco subcomplex and the complex as a whole.

https://doi.org/10.5194/egusphere-2025-5795
Preprint. Discussion started: 19 February 2026

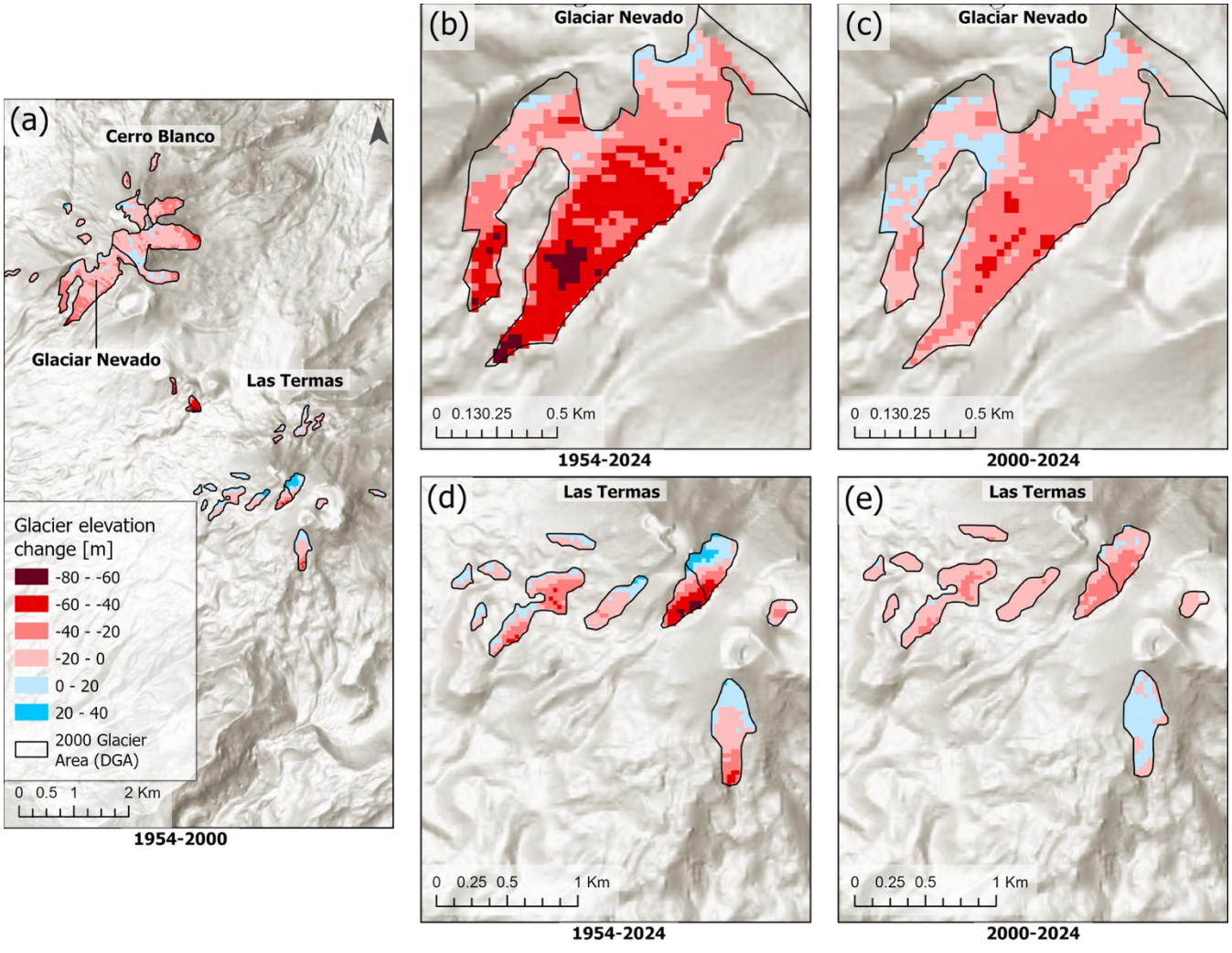

Figure 3: Glacier elevation change [m] of the Cerro Blanco and Las Termas subcomplexes on Nevados de Chillán within year 2000 glacier perimeters. A) 1954-2000 elevation changes are mapped for the entire glacier complex, whereas 1954-2024 (B and D) and 2000-2024 (C and E) changes were constrained by UAV flight limitations (Sources: Esri, TomTom, Garmin, FAO, NOAA, USGS, © OpenStreetMap contributors, and the GIS User Community | Powered by Esri).

Glacier loss was greatest near the tongue of each glacier, showing a relationship between greater glacier thinning and lower elevation. Between 2000 and 2019, the glaciers situated on the saddle between the Cerro Blanco and Las Termas subcomplexes disappeared entirely (Fig. 3). Given that we were unable to survey the northeastern aspect of the complex, the melt dynamics of those glaciers were not determined (Fig. 3). Pixels that increased in elevation were mostly clustered on the southern face of the Las Termas subcomplex.

https://doi.org/10.5194/egusphere-2025-5795
Preprint. Discussion started: 19 February 2026

Mean and median glacier thinning on the Cerro Blanco subcomplex exceeds that on the Las Termas subcomplex across all periods (Fig. 3). Furthermore, elevation loss from 2000-2024 for the two subcomplexes far exceeds that measured from 1954-2000, indicating an increase in the rate of mass loss post-2000.

We analyzed the relationship between elevation change (Δh) and pixel aspect, slope, and elevation, and found that these geographic factors only explained up to 6% ($p<0.05$) of observed elevation change, meaning that most of the variation is controlled by other factors (Appendix D). While geographic patterns vary by glacier subcomplex and by year, geographic variables had a very small and insignificant effect on glacier surface elevation change overall. We also observed significant ($p = 0.001$) spatial autocorrelation in pixels with elevation change, calculating Global Moran's I values for the glacier elevation change raster layers ranging from a minimum of 0.69 to a maximum of 0.82. Using Local Moran's I analysis, we found a high degree of clustering, i.e. pixels with high (low) elevation loss are near pixels with high (low) elevation loss (Appendix E). In other words, we found that glacier elevation loss on Nevados de Chillán is spatially coherent.

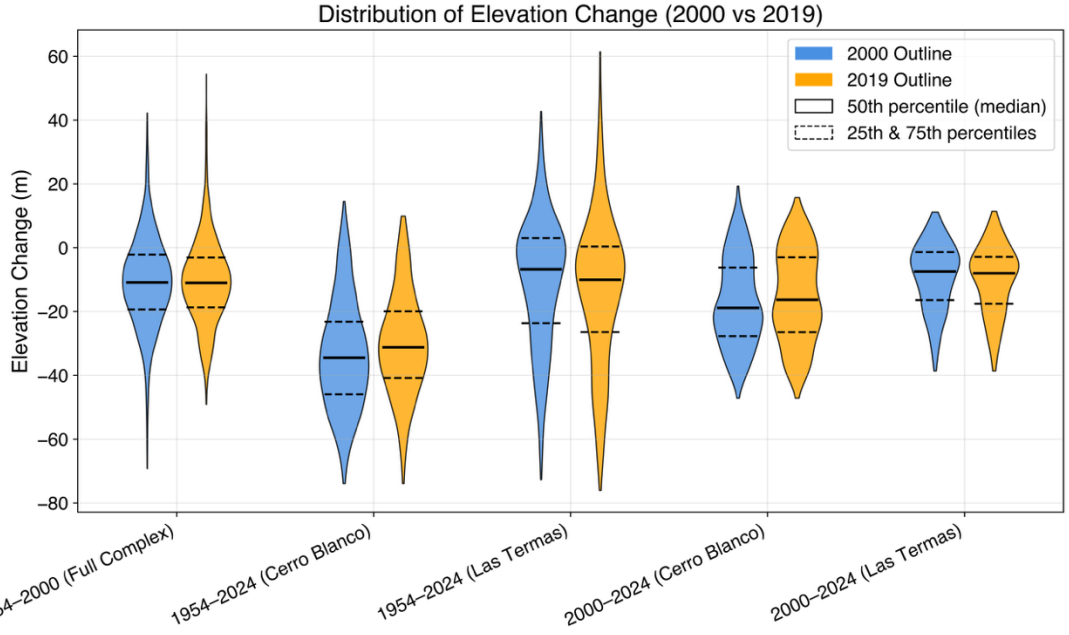

Figure 4: Distribution of glacier elevation change for the Cerro Blanco and Las Termas subcomplexes and the entire Nevados de Chillán complex with median, 25th and 75th percentiles plotted.

We also observed the impact of glacier outline choice (2000 vs 2019) on measured glacier elevation change (Fig. 4). For the full Nevados de Chillán complex, mean elevation differences were nearly identical between inventories and not significant. The Las Termas subcomplex showed slightly greater elevation loss using 2019 outlines, but the change was not significant. In contrast, the Cerro Blanco subcomplex exhibited small but significant differences: relative to SRTM, the mean difference increased from -17.0 m (2000) to -15.3 m (2019) ($t = -2.31$, $p = 0.021$), and relative to IGM, from -33.4 m to -30.3 m ($t = -3.60$, $p = 0.00033$), indicating slightly reduced apparent ice loss using the 2019 outlines (Appendix F). These results

https://doi.org/10.5194/egusphere-2025-5795
Preprint. Discussion started: 19 February 2026

demonstrate that mass balance estimates for smaller subcomplexes are more sensitive to the choice of glacier inventory, while the overall complex is largely unaffected.

4.3 Mean Mass Balance of Nevados de Chillán Complex

From 1954-2024, the Cerro Blanco subcomplex had a mean annual specific mass balance of -0.41 (-0.37) ± 0.33 m w.e. yr^{-1} within the year 2000 (2019) glacier outlines, whereas the Las Termas subcomplex had a mean annual specific mass balance of -0.13 (-0.16) ± 0.18 m w.e. yr^{-1}. More recently, from 2000-2024, the Cerro Blanco subcomplex had a mean annual specific mass balance of -0.60 (-0.54) ± 0.29 m w.e. yr^{-1} within the year 2000 (2019) glacier outlines, whereas the Las Termas subcomplex had a mean annual specific mass balance of -0.32 (-0.36) ± 0.18 m w.e. yr^{-1} within the year 2000 (2019) glacier outlines. This suggests accelerating melt for these 11 glaciers in the past 24 years when compared to the entire 70-year study period. Fig. 5 summarizes mass balance and error calculations for all time periods within both the 2000 and 2019 glacier outlines.

Mean glacier thinning of the Cerro Blanco subcomplex far exceeded that of the Las Termas subcomplex. For the entire 70-year period, Cerro Blanco lost an average of -33.43 ± 8.14 m in elevation, compared to just -8.46 ± 5.12 m on average from Las Termas (Fig. 3). The relatively higher measurement error calculated for the 1954 IGM DEM precludes precise estimations on how much of that ice loss occurred before the year 2000.

The mass balance of Glaciar Nevado, the largest glacier on Nevados de Chillán, was calculated for the entire 70-year period, in addition to the 1954-2000 and 2000-2024 sub-periods (DGA, 2014; 2022). The mean annual mass balance within the 2000 glacier extent was -0.41 ± 0.33 m w.e. yr^{-1} over the full study period (1954–2024), -0.30 ± 0.47 m w.e. yr^{-1} from 1954–2000, and -0.60 ± 0.29 m w.e. yr^{-1} from 2000–2024 (Fig. 5). The mean annual mass balance within the 2019 glacier extent was -0.37 ± 0.33 m w.e. yr^{-1} over the full study period (1954–2024), -0.27 ± 0.47 m w.e. yr^{-1} from 1954–2000, and -0.54 ± 0.29 m w.e. yr^{-1} from 2000–2024 (Fig. 5). These results suggest an increasing rate of glacier mass loss over time. The magnitude of glacier loss from 1954-2000 was within the range of measurement uncertainty, however glacier loss was significant within both the 2000 and 2019 glacier areas from 1954-2024 and 2000-2024.

https://doi.org/10.5194/egusphere-2025-5795
Preprint. Discussion started: 19 February 2026

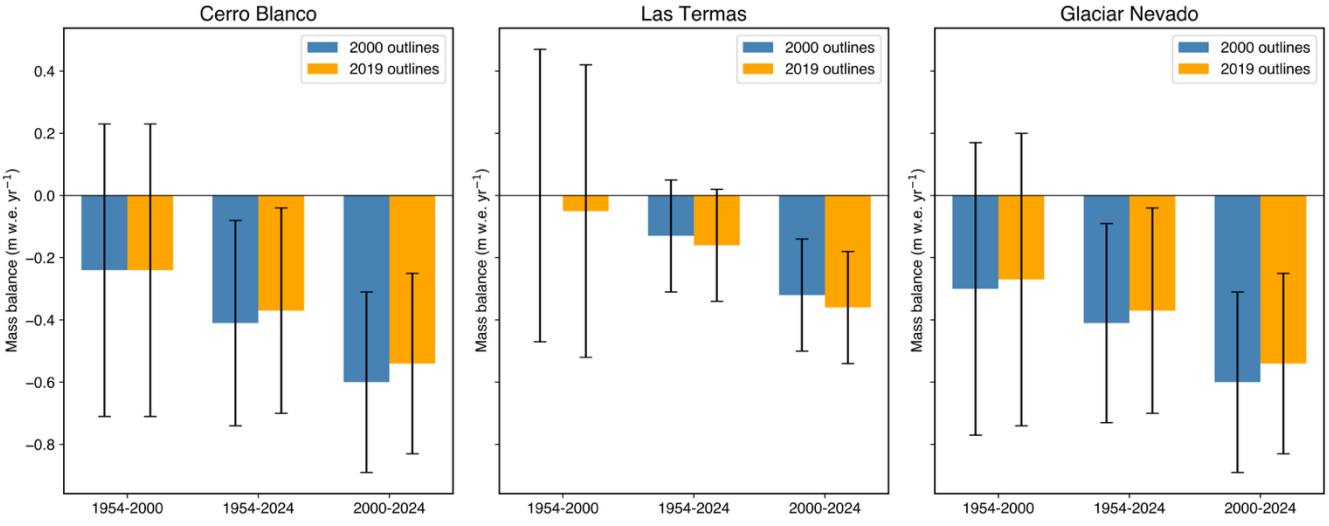

Figure 5: Box plot of mean annual glacier mass balance and whiskers showing error calculations for both the 2000 (blue) and 2019 (orange) glacier outlines.

In summary, mean annual specific mass balance decreased over time for both the Cerro Blanco and Las Termas subcomplexes, as well as for Glaciar Nevado. Mass balance was negative but was smaller than the measurement uncertainty for the 1954-2000 study period, however, due to the lower resolution of historic elevation data. NMAD also exceeded the signal of glacier mass balance from 1954-2024 for the Las Termas subcomplex due to the relatively small signal of glacier loss.

4.4 Hydroclimatic Trends

We found that annual cumulative precipitation decreased by an average of 22.20 mm yr^{-1} ($p = 8.85 \times 10^{-3}$) at the Diguillín meteorological station, and by -44.86 mm yr^{-1} ($p = 1.18 \times 10^{-5}$) at the Las Trancas station from 1980-2020 (Fig. 6 A and B). The year 2007 was identified as a change point in both time series, indicating a shift in the regional precipitation regime beginning that year (Fig. 6 A and B). Corroborating this point, the five lowest precipitation years occurred since 2007 for the Las Trancas station, while four of five occurred in 2007 or later for the Diguillín station. By contrast, the five highest precipitation years for both stations occurred before 2007.

https://doi.org/10.5194/egusphere-2025-5795
Preprint. Discussion started: 19 February 2026

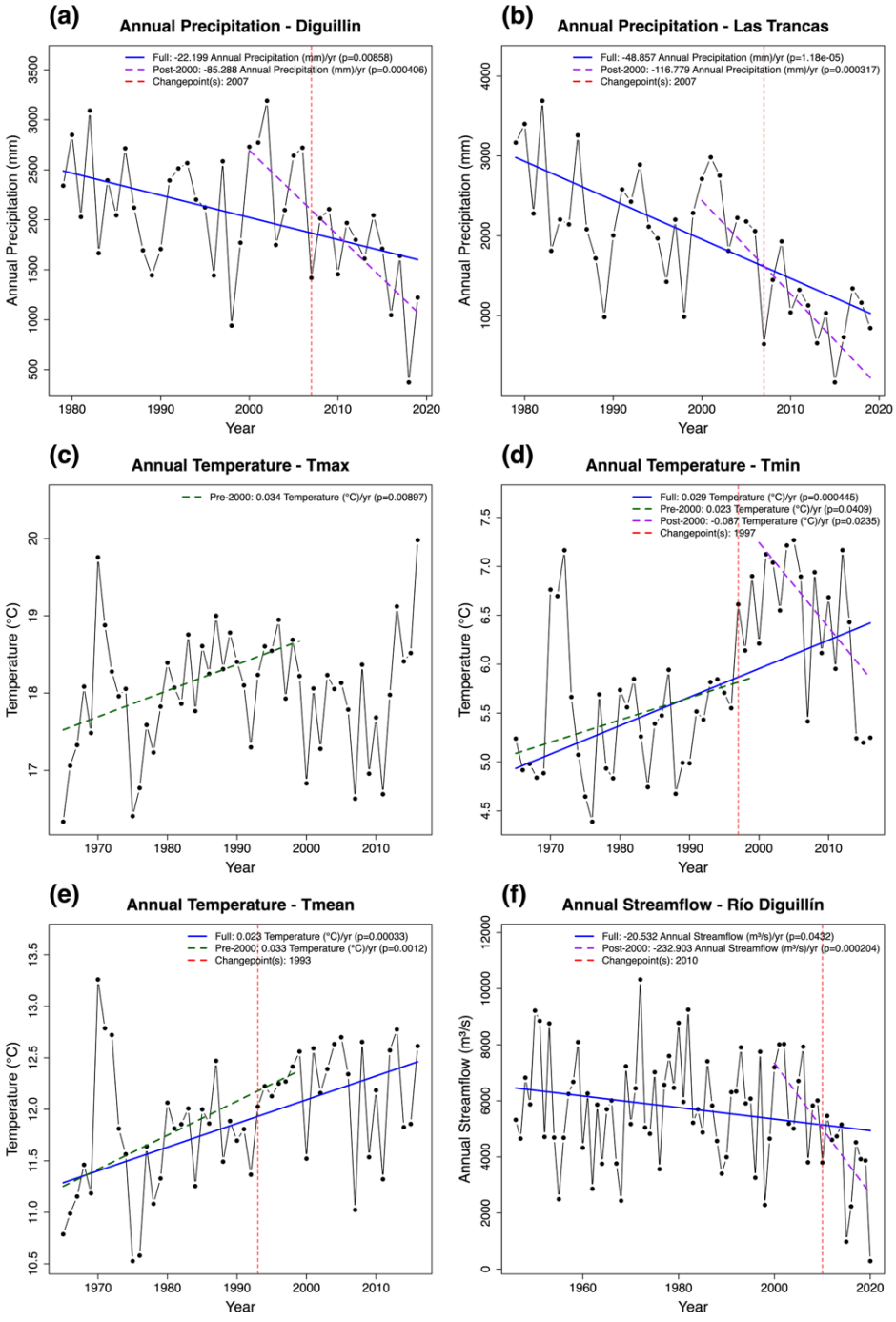

345 **Figure 6: Change-point and trend analysis of annual cumulative precipitation and streamflow and mean annual temperature at the Las Trancas and Diguillín meteorological stations. Annual cumulative precipitation decreased at both Diguillín and Las Trancas stations ($p<0.05$).**

https://doi.org/10.5194/egusphere-2025-5795
Preprint. Discussion started: 19 February 2026

Since no temperature data were available for Las Trancas, maximum, minimum, and mean temperature was analyzed for the Diguillín station alone (Fig. 6 C, D, E). Average annual minimum daily temperatures increased by 0.029°C yr^{-1} ($p = 4.45 \times 10^{-4}$) and average annual mean daily increased by 0.023°C yr^{-1} ($p = 3.30 \times 10^{-4}$) (Fig. 6 D and E). Average annual maximum temperatures showed no significant trend (Fig. 6. C). Change points occurred in 1993 for mean and 1997 for minimum annual average temperatures. Unlike the precipitation series where nine out of ten of the lowest precipitation years have occurred since 2007, the five years with highest mean temperature were more spread throughout the time series (Fig. 6 D and E). Streamflow was also analyzed for Río Diguillín station, with cumulative annual streamflow decreasing by -20.53 $m^3\ s^{-1}\ yr^{-1}$ ($p=0.04$) over the full time series. Analysis of post-2000 average cumulative annual streamflow indicated dramatic reductions, with streamflow decreasing by -232.90 $m^3\ s^{-1}\ yr^{-1}$ ($p = 2.04 \times 10^{-4}$), representing a >1000% increase in the rate of streamflow decline. The timeseries of annual average minimum, mean, and maximum air temperatures and streamflow, and annual cumulative precipitation, are shown above in Fig. 6.

Finally, we analyzed changes in summertime (DJF) temperature (Fig. 7), precipitation (Fig. 8), and streamflow (Fig. 9). December (Fig. 7 A and C) and January (Fig. 7 D and F) daily minimum and mean temperatures increased significantly over the study period. December daily minimum temperatures (Fig. 7 A) experienced a change point in 1995, while January (Fig. 7 D) and February (Fig. 7 G) minimum temperatures experienced a change point in 2001. Maximum daily January temperatures (Fig. 7 E) experienced a change point in 1983, while mean daily January (Fig. 7 F) and February (Fig. 7 I) temperatures experienced change points in 2004 and 2001, respectively. Post-2000 daily maximum (Fig. 7 E) and mean (Fig. 7 F) January temperatures increased significantly, compared to the full timeseries trend.

https://doi.org/10.5194/egusphere-2025-5795
Preprint. Discussion started: 19 February 2026

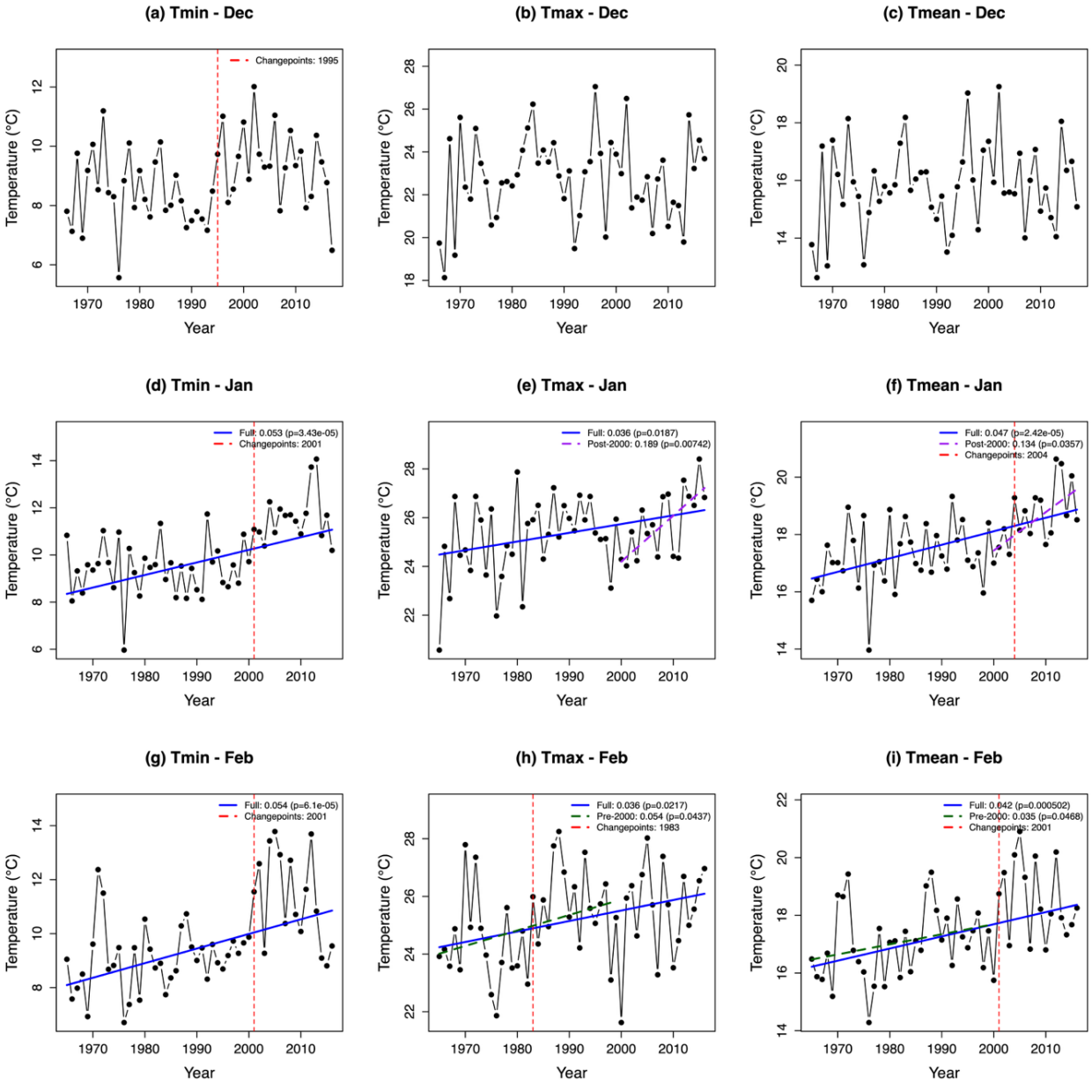

Figure 7: Change-point and trend analysis of monthly summertime (DJF) mean annual temperature downstream of Nevados de Chillán.

Interestingly, we find that summertime precipitation has not changed significantly over the study period, and no change points were detected (Fig. 8). This suggests that, while annual cumulative precipitation has decreased significantly, summertime precipitation has not, meaning that precipitation changes are greatest in the accumulation season rather than the ablation season.

https://doi.org/10.5194/egusphere-2025-5795
Preprint. Discussion started: 19 February 2026

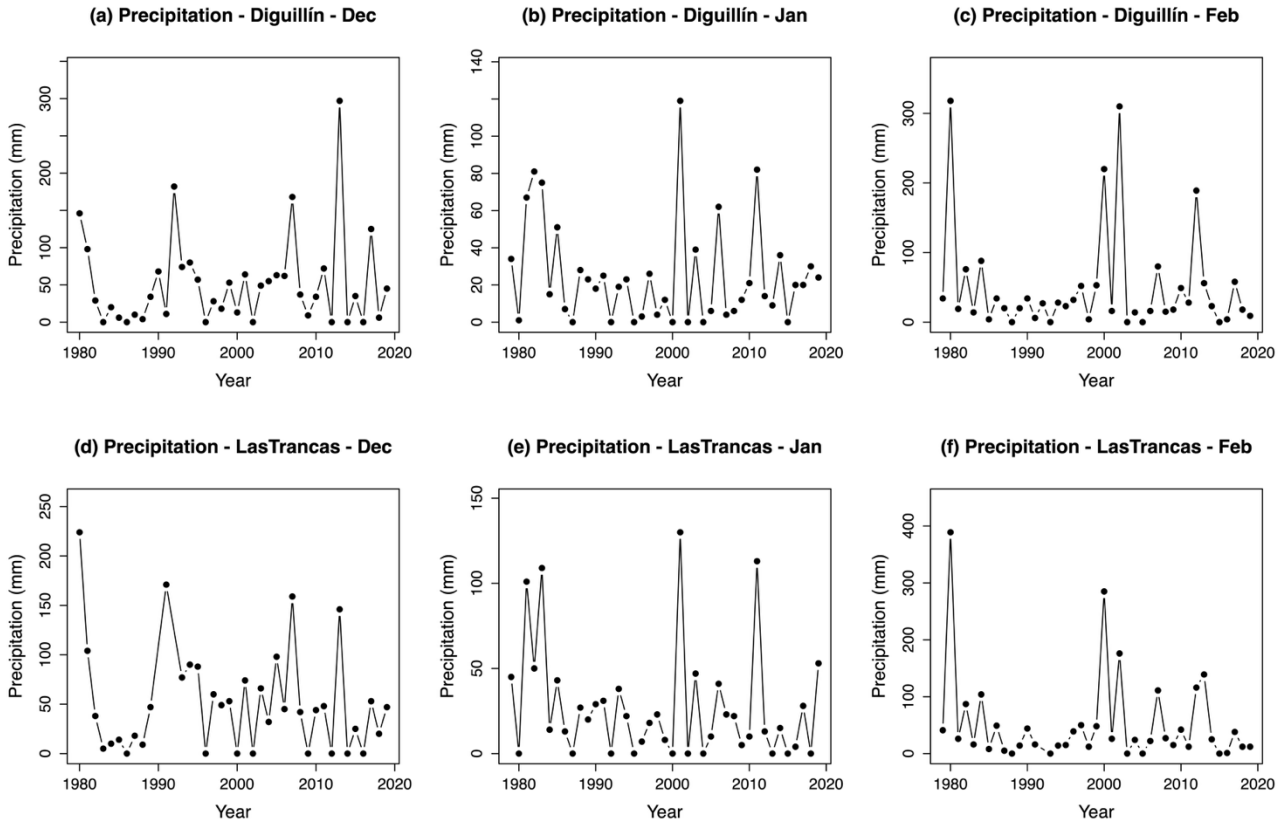

Figure 8: Change-point and trend analysis of monthly summertime (DJF) cumulative precipitation downstream of Nevados de Chillán.

375 December (Fig. 9 A) and January (Fig. 9 B) streamflow, on the other hand, have decreased significantly over the full study period, and post-2000 February streamflow has also decreased significantly (Fig. 9 C). February represents a month when all seasonal snow has typically melted off, meaning that significant post-2000 decreases in streamflow could be a result of decreased glacier melt. A change point was identified for December streamflow in 1988 (Fig. 9 A).

https://doi.org/10.5194/egusphere-2025-5795
Preprint. Discussion started: 19 February 2026

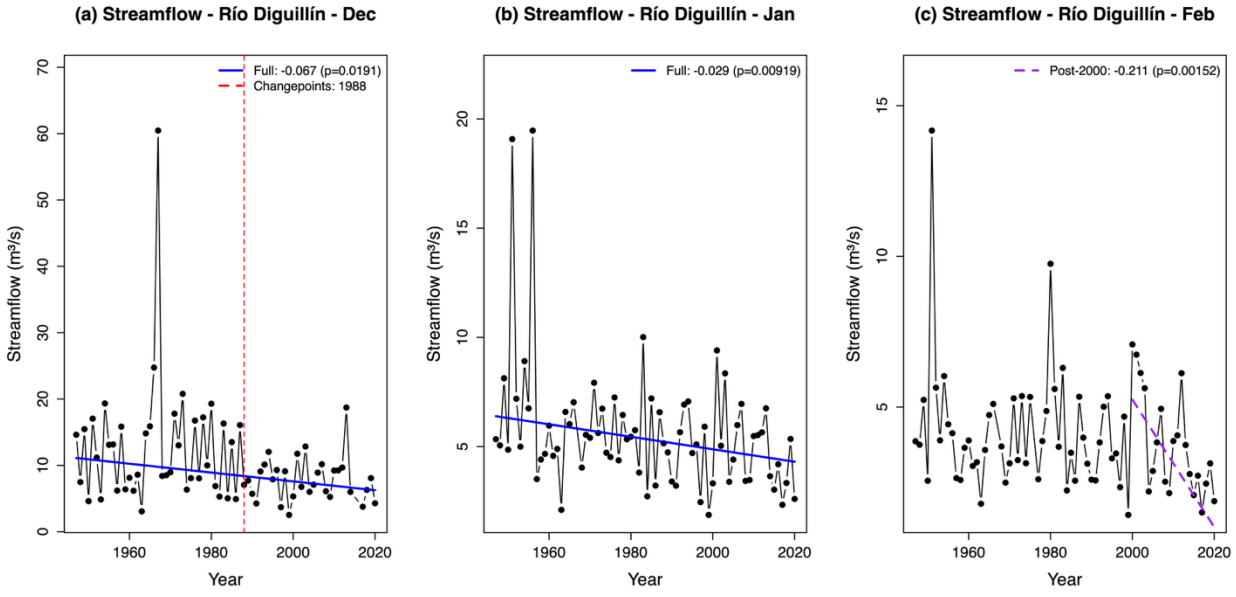

Figure 9: Change-point and trend analysis of monthly summertime (DJF) cumulative streamflow downstream of Nevados de Chillán.

Significant increases in post-2000 January daily maximum (Fig. 7 E) and mean (Fig. 7 F) temperatures, and post-2000 decreases in February daily streamflow (Fig. 9 C), may both be related to trends accelerating post-2000 glacier loss observed in this paper. Increasing summertime temperatures accelerate glacier melt and are reflected in our increasingly negative glacier mass-balance calculations. The decrease in post-2000 February streamflow (Fig. 9 C) could indicate that the glaciers on Nevados de Chillán passed peak water, meaning that despite their increasing rate of glacier mass loss over time, post-2000 streamflow contributions have decreased (Huss and Hock, 2018). An in-situ or modeling analysis of glacier melt contributions would be necessary to confirm this attribution, however.

5 Discussion

5.1 Findings and Implications

This study reports a negative mass-balance trend on average across the study period across the entire Nevados de Chillán complex. For the glaciers surveyed by UAV, we observed a significant increase in glacier loss rate for the Cerro Blanco and Las Termas subcomplexes from 2000-2024 compared to 1954-2000. While these results provide the first geodetic mass-balance calculations for the full Nevados de Chillán complex, previous work by the DGA reports the mass balance of Glaciar Nevado from 2021-2022 and 2023-2024 (DGA 2022; 2024). These multi-decadal trends are substantially smaller in magnitude than short-term estimates reported by the DGA for 2021–2022 and 2023–2024, which were derived from four ablation stakes and partial (40–60%) glacier UAV LiDAR coverage. The DGA's single-year measurements suggest extreme annual losses

https://doi.org/10.5194/egusphere-2025-5795
Preprint. Discussion started: 19 February 2026

(~–8 m w.e. in 2021–2022 and ~–7 m in 2023–2024), whereas their LiDAR estimates ranged from pronounced thinning (–5.37 m) to near-zero balance (+0.02 m), the latter likely reflecting an above-average snowfall year. The larger magnitude of the DGA's values likely stems from differences in temporal scale (single-year vs. this study's multi-decadal analysis), spatial coverage (40-60% versus full glacier coverage), and limitations of spatial interpolation of point-scale measurements, whereas our record captures multi-decadal averages over the full complex. Here, we observed localized thinning of -40 to -60 m from 2000-2024 (Fig. 3), confirming that multi-meter annual losses can occur but do not represent long-term trends. Overall, the results from our complex-wide long-term glacier analysis are more consistent with regional geodetic studies across the southern Andes, suggesting that Nevados de Chillán's glaciers are responding in line with broader regional patterns.

Regional-scale geodetic glacier mass-balance studies generally align more closely with our findings at Nevados de Chillán than the short-term DGA analyses described above. The Nevados de Chillán complex is included in broader studies conducted by Dussaillant et al. (2020), Zemp et al. (2019), and Braun et al. (2019). Dussaillant et al. (2019) measured a mass balance ranging from -0.31 ± 0.19 m w.e. yr^{-1} in the Central Andes and -0.57 ± 0.22 m w.e. yr^{-1} in Northern Patagonia, between 2000-18, with Nevados de Chillán located near the transition from the Central Andes to Northern Patagonia. Braun et al. (2019) reported mass balance of just -0.05 ± 0.09 m w.e. yr^{-1} over 2000-2011/15 for the Chilean Lakes District (~35-42°S), also encompassing the study area, whereas Zemp et al. (2019) reported the most negative mass balance of -1.18 ± 0.38 m w.e. yr^{-1} for 2006-2016 over the Southern Andes. Nevados de Chillán lies within the study areas of these regional assessments, and our mass balance estimates are generally consistent with the ranges reported at the regional scale, despite differences in temporal coverage, glacier extent, and methodology—including whether area change is considered. These results highlight the strong spatial variability of glacier mass balance in the Andes, emphasizing that local studies like ours are essential for accurately constraining basin- and glacier-scale changes. Mountain-to-mountain variability, differences in observational methods, and temporal coverage all significantly influence mass balance estimates, making site-specific analyses critical for understanding glacier response and for informing local hydrological management.

Though spatially and temporally heterogeneous, south-central Chile is experiencing both warming and drying trends on average as indicated by detailed analyses performed by Shumacher et al. (2020) and Lagos-Zúñiga et al. (2024) and supported by the analyses herein. The trends observed for the Las Trancas and Diguillín stations are in line with precipitation decreases and temperature increases observed in previous studies. For example, Martínez-Retureta et al. (2021) find similar trends from 1976–2016 in the Muco basin to the south of the study area. Climate change, in addition to the negative Pacific Decadal Oscillation phase and the El Niño phase, are all shown to contribute to the observed warming and drying trends (Boisier et al., 2015; Cordero et al., 2024; Garreaud et al., 2017; 2024). In particular, the Central-Andes Mega Drought caused accelerated decreases in mean annual precipitation (Boisier et al., 2015). Caro et al. (2024) found that climate presents higher explanatory power than geographic variables in the Andes, with precipitation exerting the strongest control on glacier mass balance. While our finding that annual cumulative precipitation is decreasing echoes previous studies, our conclusion that summertime

https://doi.org/10.5194/egusphere-2025-5795
Preprint. Discussion started: 19 February 2026

precipitation has not changed significantly (Fig. 8) disagrees with previous work (Garreaud et al., 2020; Rubio-Álvarez and McPhee, 2010).

Average annual minimum and mean temperatures were shown to increase significantly for the Diguillín station near Nevados de Chillán (Fig. 7), while trends in maximum average annual temperatures were not significant (Fig. 6). We found that January and February minimum, mean, and maximum monthly temperatures are increasing substantially for the station nearest to Nevados de Chillán (Fig. 7 D-I). Post-2000 mean and maximum monthly temperature increases have accelerated in February (Fig. 7 H-I). Caro et al. (2024) also found that temperature increases have accelerated in recent years compared to historic temperature regimes, though over a different period than our analysis, finding that mean annual temperatures increased by 0.3°C from 2010-2014, compared to 1979-2014 (Caro et al., 2024). In addition to a shift in precipitation from snowfall to rainfall, extreme droughts are increasing in south-central Chile (Poveda et al., 2020).

The analysis herein indicated that streamflow decreased over the full study period (Fig. 6 F), with significant reductions in post-2000 February and annual cumulative discharge (Fig. 9 C and Fig. 7 F). This decline is consistent with the glaciers on Nevados de Chillán having passed peak water, meaning that meltwater contributions are now decreasing despite accelerated mass loss (Huss and Hock, 2018). Although rising January and February temperatures (Fig. 7 D-I) have increased the rate of vertical melt (m w.e. yr^{-1}), the glaciers have lost substantial surface area and total ice volume, so a faster rate of thinning is occurring over a much smaller ice reservoir. As a result, the total volume of melt available for runoff decreases, even while the calculated mass balance becomes more negative. An in-situ or modeling analysis of glacier melt contributions would be necessary to confirm that streamflow reductions are attributable to glacier mass loss, as opposed to other hydrological inputs, but our findings suggest that glacier retreat has progressed to a stage where declining ice volume has begun to reduce relative meltwater contributions to streamflow.

Another potential attribution for glacier mass patterns on Nevados de Chillán is volcanic activity. It is yet unknown whether ice-lava interaction and/or the impact of thin deposition of volcanic tephra decreasing the albedo of glacier surface have impacted glacier melt on the Nevados de Chillán complex. Volcanic activity on the Las Termas subcomplex increased dramatically from 2016-2019 (Global Volcanism Program, 2022). More recently, from June-October 2022, over 1,000 explosive volcanic events were reported from the Nicanor crater on the Las Termas subcomplex (Servicio Nacional de Geología y Minería, 2025; Global Volcanism Program, 2022). Some of these events triggered pyroclastic flows and avalanches, as well as substantial debris deposition on glacier surfaces (Lizama et al., 2025). Debris cover is a rapidly developing area of glacier research–in the case of thin and/or discontinuous debris, ablation typically increases due to the lower albedo of debris (rock, sand, dust, or ash) compared to snow and ice (Brock et al., 2007). The decreased albedo causes an increase in the ratio of radiation absorbed to reflected, causing an increase in glacier surface melt (Rivera et al., 2006; Wigmore and Mark, 2017; Rounce et al., 2021; Bisset et al., 2022; Rossini et al., 2023). Given the similar flow topography of pyroclastic

https://doi.org/10.5194/egusphere-2025-5795
Preprint. Discussion started: 19 February 2026

and lahar deposits, and debris-covered glaciers, it is difficult to tell from remote imagery whether some glaciers on the Las Termas subcomplex are now debris-covered or have disappeared altogether. Future work should be done to determine the extent debris cover on Nevados de Chillán and the impact on glacier mass balance.

5.2 Limitations and Assumptions

One limitation of the work herein was the use of two glacier polygon datasets, corresponding to the years 2000 and 2019. In the absence of area estimates corresponding to each year within the study period, we estimated geodetic mass balance using 2000 and 2019 glacier areas. Glacier mass balance calculations herein were thus reliant on vertical ice thinning measurements rather than glacier area change. As a result, mean annual glacier mass balance estimates were conservative for 1954-2000, as glacier area likely decreased substantially over the study period, while our use of the year 2000 glacier outlines assumed a constant glacier area. We produced 2000-2024 annual mass balance estimates with both the 2000 and 2019 areas, thus providing a range of likely values. For years after 2019, mean annual mass balance estimates were conservative as they do not consider recent glacier area loss. While this study provides valuable insight into retreat rates, future studies would benefit from exploring glacier mass balance on finer time resolutions to isolate the impacts of volcanic eruptions, tectonic uplift, anthropogenic climate change, and regional climate variability on interannual glacier mass balance.

The reliance on just three DEMs to reconstruct 70 years of glacier mass balance does not illuminate interannual fluctuations (Rabatel et al., 2017). Thus, our calculation of mean annual mass balance from total estimated mass balance should be used with caution (Rabatel et al., 2017). This approach, however, is widely accepted for geodetic mass balance estimates of mountain glaciers, given the scarcity of DEM products for these regions (e.g. Farías-Barahona et al., 2019). Similar studies show high agreement between geodetic measurements from remotely sensed DEMs and in-situ mass-balance measurements (Beraud et al., 2022). Thus, remotely sensed DEMs provide an excellent option to compute glacier-wide mass balance in the absence of detailed in-situ measurements.

While differencing DEMs enabled the calculation of glacier mass balance, estimating geodetic mass balance relied on the established estimation of mean glacier density of 850 kg m^{-3}, rather than accounting for variations in density across glacier area and time (Huss, 2013; Farías-Barahona et al., 2019). However, Huss (2013) indicated that errors inherent to ice density assumptions decrease with longer-scale geodetic studies. In the case of this study, our 70-year analysis period far exceeds the suggestion by Huss (2013) of >5-10 years to reduce mean glacier density estimation error.

Another limitation of this study is that only the western/southwestern glaciers were surveyed in 2024 with the UAV campaign, due to logistical and weather limitations. While we computed mass balance for all inventoried glaciers on Nevados de Chillán between 1954-2000, we were only able to provide mass balance for 11 of the 28 inventoried glaciers post-2000. Mass balance

https://doi.org/10.5194/egusphere-2025-5795
Preprint. Discussion started: 19 February 2026

from 1954-2000 and 2000-2024 was only compared for these 11 glaciers for the sake of consistency, whereas complex-wide mass balance was only computed for 1954-2000.

The existing studies on Nevados de Chillán exclusively focus on the clean-ice, failing to account for the presence of debris cover which is evident on the complex, and is likely due to both rock slides and eruptions from the Las Termas subcomplex depositing volcanic ash, tephra, and other debris on the glacier surfaces (Zenteno et al., 2004; Caro, 2014). Frequent eruption events make it particularly difficult to distinguish pyroclastic and lahar deposits from debris covered glaciers. Due to the difficulty in accurately delineating current debris covered glacier extent, in addition to the difficulty of distinguishing snow patches from glacier ice, we did not estimate current glacier extent. By relying on the 2019 glacier outline as our most recent glacier area, we likely underestimated glacier area closer to initial DEM date (i.e. 2000-2019) and overestimated recent (i.e. post-2019) glacier area. Additionally, this geodetic mass balance approach does not remove debris thickness from glacier surface height estimation and instead just measures the ground surface height within 2000 and 2019 glacier boundaries, respectively. As a result, the results presented herein may underestimate glacier loss in cases where the actual glacier surface is covered by debris.

An additional limitation of this study is due to the active volcanic and tectonic activity on Nevados de Chillán, as it pertains to our comparison of 2024 DEMs with 2000 and 1954 DEMs. First, in 2010 an 8.8 moment magnitude [M_w] earthquake in the neighboring region of Maule caused plate subsidence in the Chilean central valley, and uplift in the Andes Mountain range of up to 20 cm, from 33 to 40°S (Li et al., 2017). In effect, our 2024 UAV DEM is subject to additional uncertainty after co-registration due to possible uplift of the Nevados de Chillán volcanic complex. Given that a strong glacier melt signal was measured between 2000-2024 in this study, the effect of tectonic uplift on our 2024 DEM would imply that we may underestimate post-2000 glacier melt. Additionally, studying the most recent active period of Nevados de Chillán from January 2016-2023, Lizama et al. (2025) reported that there was a period of either no change or slight topographic subsidence during the first three years of the eruption, with a maximum subsidence of 0.8 cm yr^{-1} measured. This period was followed by significant uplift from 2019-2022, with stations ranging from a total observed vertical displacement of ~5-25 cm (Lizama et al., 2025). This recent uplift was attributed to increased magma flow from a deeper to a shallower reservoir (Lizama et al., 2025). Importantly, this implies that surface elevation presented in our 2024 UAV DEMs may further underestimate glacier surface elevation loss. To summarize, both earthquake and volcanic activity in the study area has likely resulted in a net uplift of between ~0-45 cm in Nevados de Chillán's topography since the year 2000.

Although the assumptions discussed above introduce some uncertainty, because tectonic uplift and supraglacial debris deposition likely contributed to increases in surface elevation, the reported estimates of mean glacier loss should be considered conservative, potentially underrepresenting the true extent of glacier volume loss. This finding highlights the challenging nature of applying glacier mass balance analyses to glaciated volcanic environments. These settings are rarely considered in

https://doi.org/10.5194/egusphere-2025-5795
Preprint. Discussion started: 19 February 2026

the existing literature, emphasizing both the novelty of this study and the need for further research focused on glaciers in volcanic regions.

6 Conclusion

This study provides the first long-term geodetic mass balance record for the glaciers of the Nevados de Chillán volcanic complex in south-central Chile, directly addressing the need to quantify how glacier mass loss has evolved in this region. Our 70-year record shows that glaciers across the complex have experienced sustained and accelerating mass loss since 1954, with greater losses on the Cerro Blanco subcomplex than on Las Termas. From 1954–2000, the full complex lost ice at a mean rate of −0.20 ± 0.47 m w.e. yr^{-1}, and losses intensified after 2000. From 1954-2024 we observed a mean annual mass balance of -0.41 (-0.37) ± 0.33 m w.e. yr^{-1} for the Cerro Blanco subcomplex, versus -0.13 (-0.16) ± 0.18 m w.e. yr^{-1} for the Las Termas subcomplex, within the 2000 (2019) glacier outlines, illustrating that recent glacier retreat is not uniform across the complex and that glacier loss has accelerated since 2000.

By establishing the magnitude and spatial variability of glacier mass loss at Nevados de Chillán, the work herein provides a benchmark against which future change can be assessed and offers a necessary foundation for understanding downstream implications. This study found that declining summer streamflow coincided with accelerated glacier loss, however, quantifying the contribution of glacier melt to river discharge remains a key task for future studies. Our results clarify the rate at which glacier volume is disappearing on Nevados de Chillán—supplying critical data to support water management and drought mitigation efforts.

Code and Data availability

The data and code utilized in this paper can be found at https://github.com/millie-spencer/Glacier-DEM-coregistration-and-MB and are hosted at: DOI: 10.5281/zenodo.17664874

Author contribution

MS, RC, EM, and AF designed the fieldwork plan. MS and RC carried out the fieldwork and processed the UAV images. AF provided the IGM DEM and advised research methodology. MS and ET developed model code and performed DEM analysis. MS produced the figures and prepared the manuscript with contributions from all co-authors.

Competing interests

The authors declare that they have no conflict of interest.

https://doi.org/10.5194/egusphere-2025-5795
Preprint. Discussion started: 19 February 2026

Acknowledgments

Thank you to my mentors at the University of Colorado, Boulder, Universidad de Chile, Universidad de Concepción, and Universidad Católica de la Santísima Concepción for hosting me over the past years.

Financial Support

This research was funded by the National Science Foundation International Research Experience for Students Program (award #1954140); the Consortium of Universities for the Advancement of Hydrologic Science, Inc. (CUAHSI) Pathfinder Fellowship; the Fulbright Chile Science Initiative; the University of Colorado, Boulder George R. Aiken Graduate Fellowship, Mabel Duncan Award, and Graduate and Professional Student Government Travel Grant; Agencia Nacional de Investigación (ANID)-FONDECYT 1201429, 1252044, and ANID-ANILLO 210080.

Appendix A: UAV DEM of Cerro Blanco co-registration to SRTM DEM result

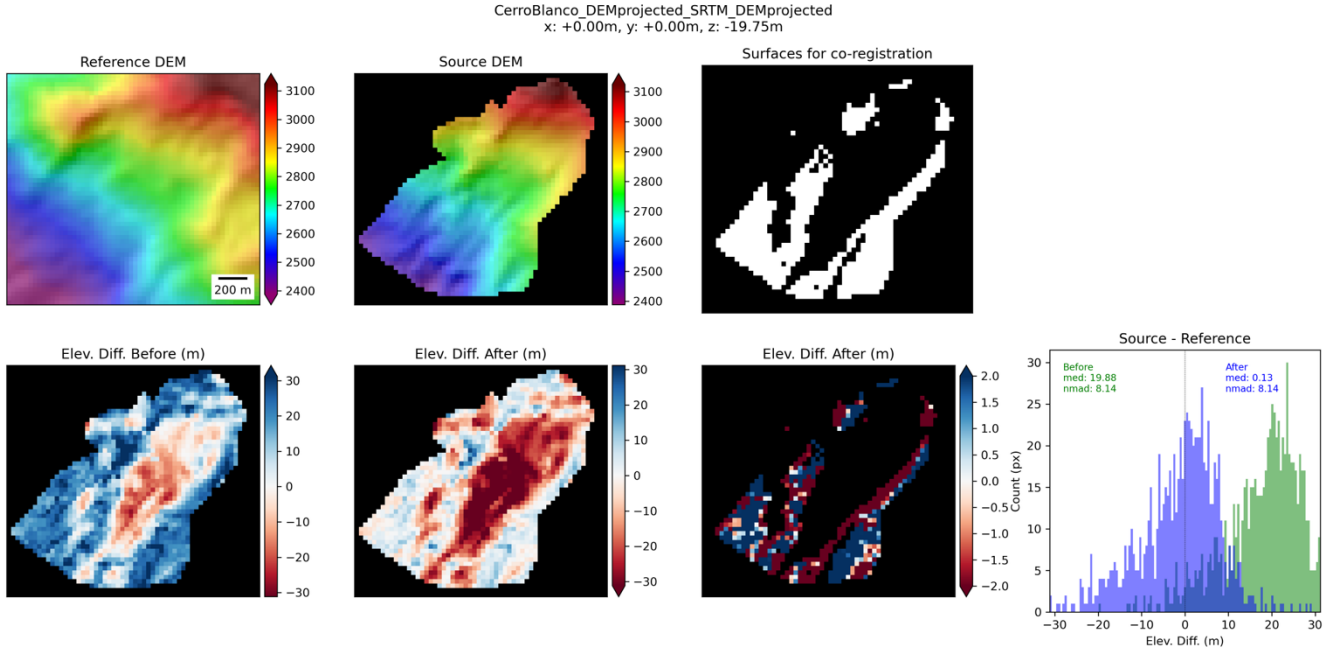

Figure A1: The process and output of co-registering the UAV DEM of Cerro Blanco to the SRTM DEM.

Appendix B: UAV DEM of Las Termas co-registration to SRTM DEM result

https://doi.org/10.5194/egusphere-2025-5795
Preprint. Discussion started: 19 February 2026

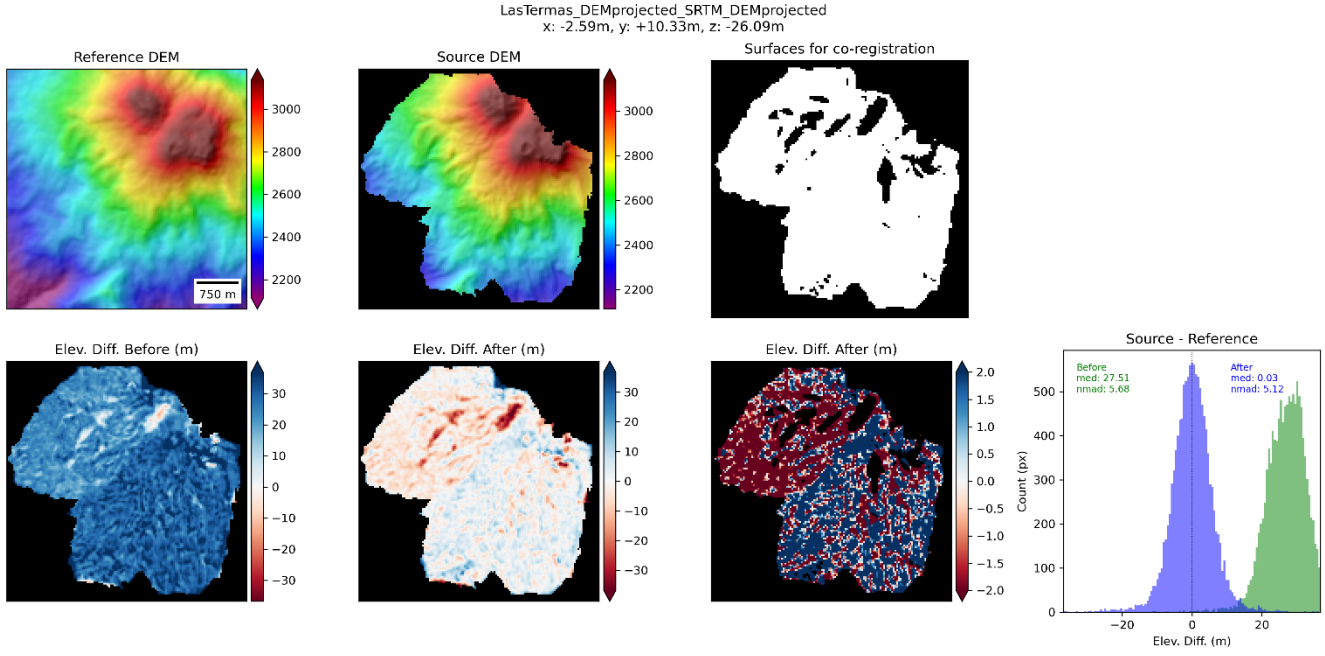

Figure B1: The process and output of co-registering the UAV DEM of Las Termas to the SRTM DEM.

Appendix C: IGM DEM co-registration to SRTM DEM result

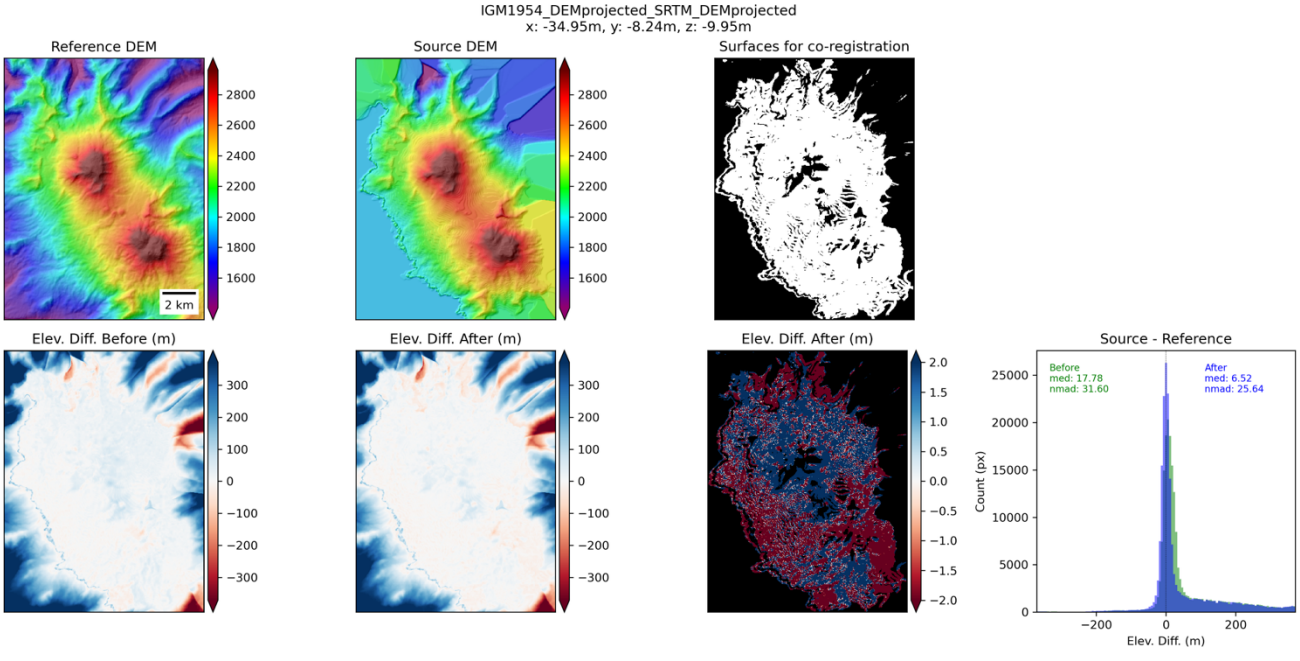

Figure C1: The process and output of co-registering the IGM DEM of Cerro Blanco to the SRTM DEM.

https://doi.org/10.5194/egusphere-2025-5795
Preprint. Discussion started: 19 February 2026

Appendix D: Influence of elevation, slope, and aspect on glacier loss

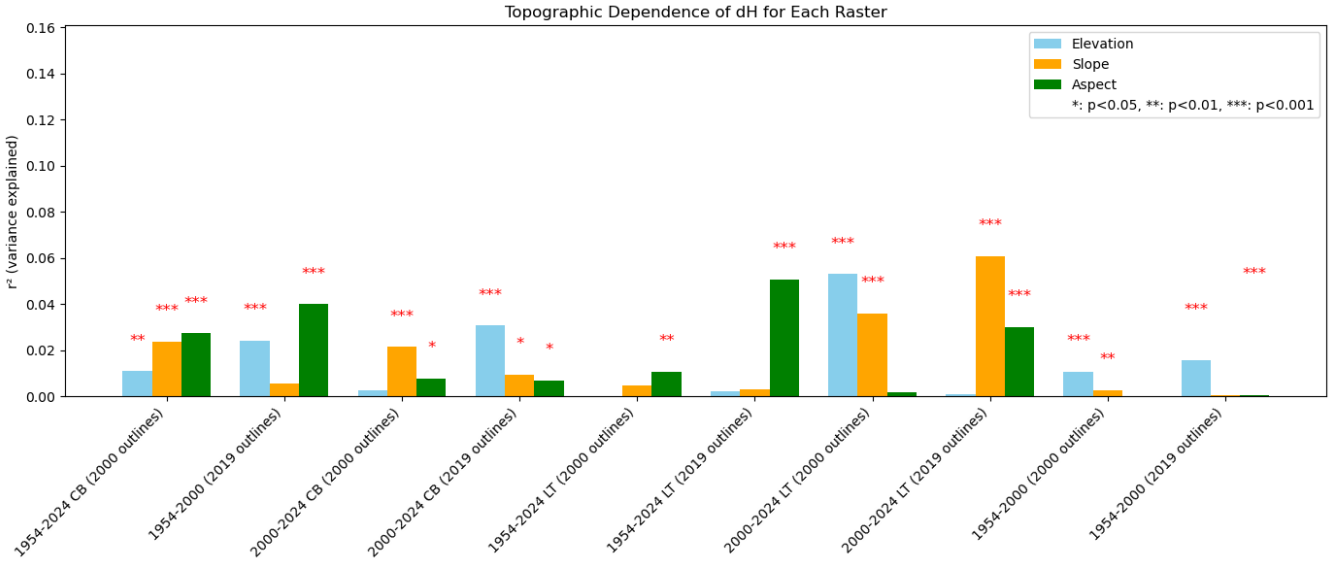

Figure D1: Statistical analysis of geospatial variable (elevation, slope, and aspect) influence on glacier thinning.

Appendix E: Global Moran's I test of spatial autocorrelation

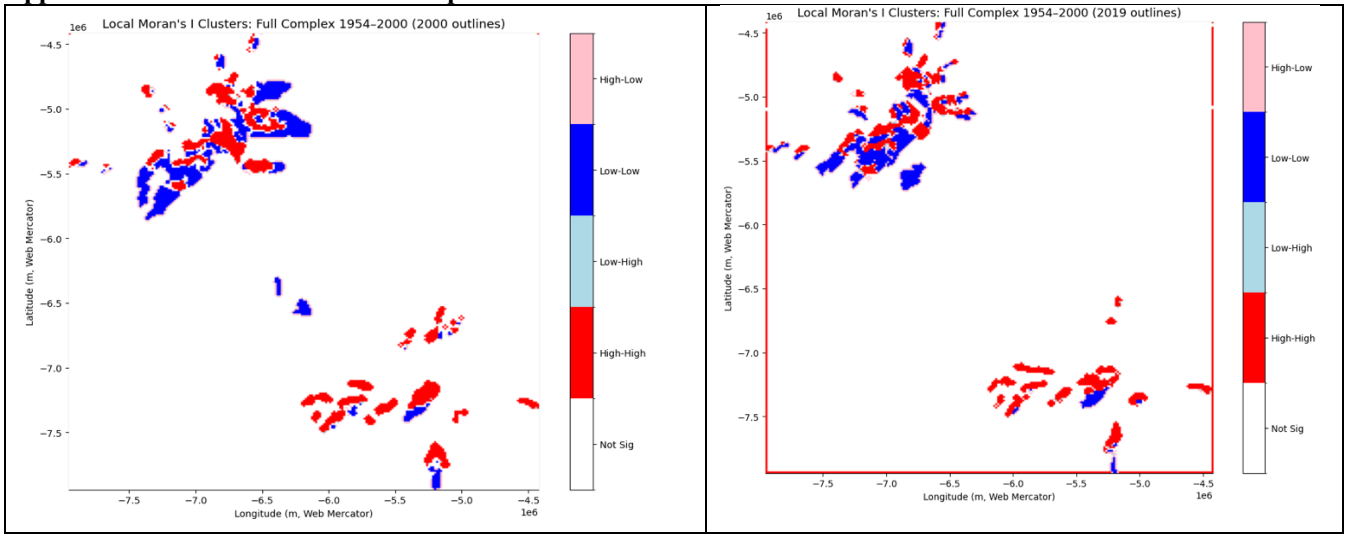

https://doi.org/10.5194/egusphere-2025-5795
Preprint. Discussion started: 19 February 2026

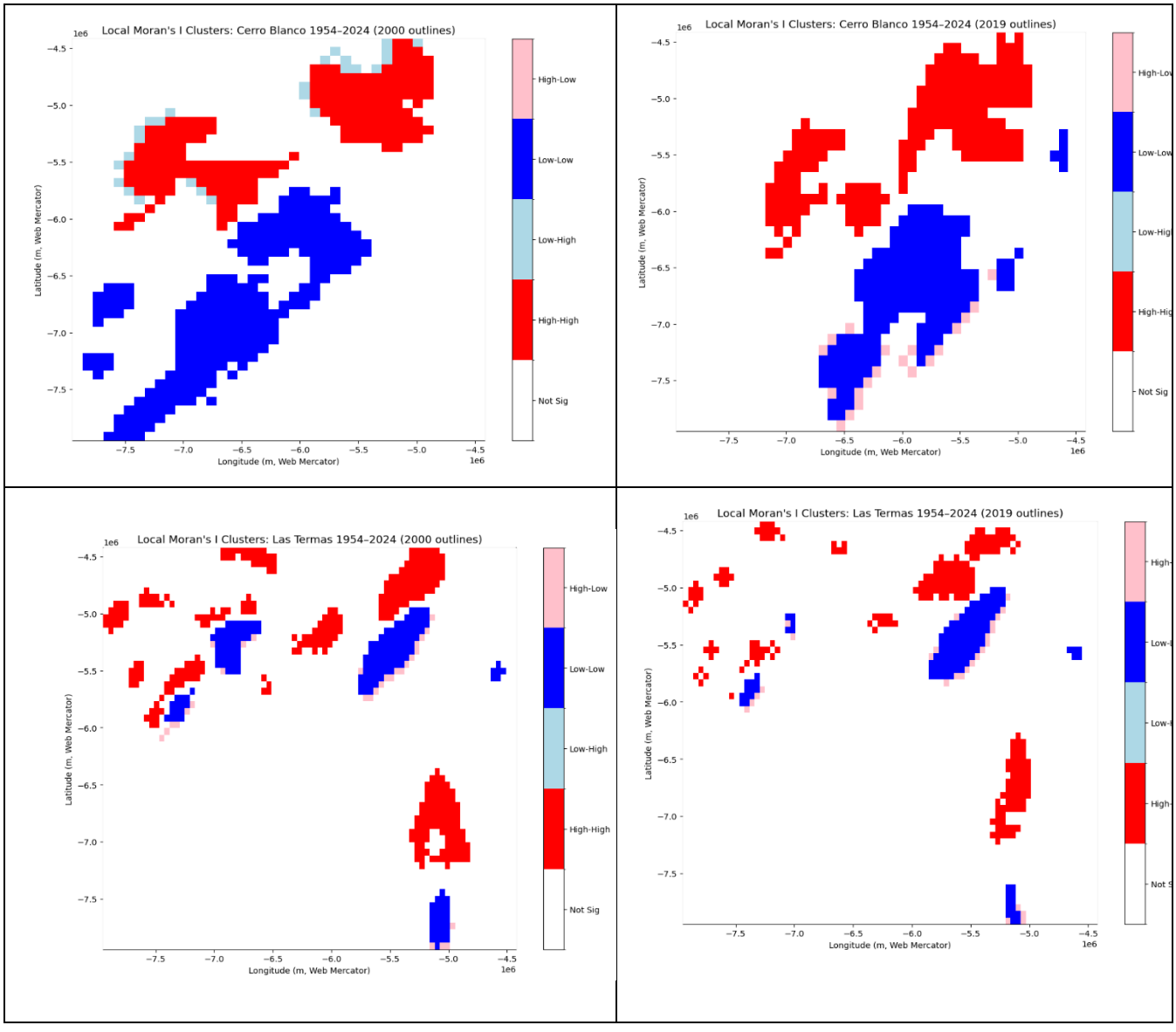

https://doi.org/10.5194/egusphere-2025-5795
Preprint. Discussion started: 19 February 2026

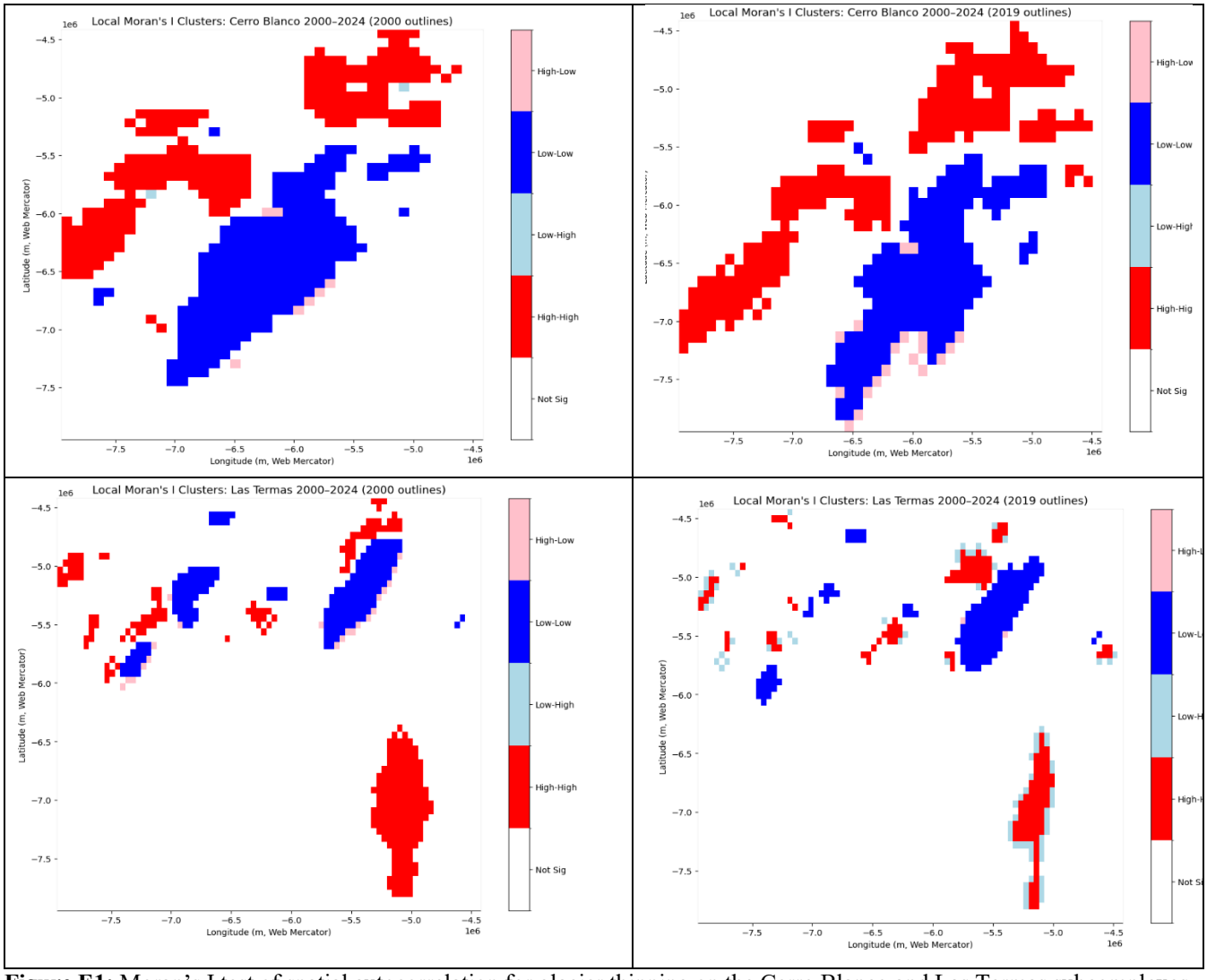

595 **Figure E1:** Moran's I test of spatial autocorrelation for glacier thinning on the Cerro Blanco and Las Termas subcomplexes.

Appendix F: Table summarizing impact of glacier inventory (2000 versus 2019 glacier outlines) on elevation loss (Δh) calculations

Raster_base	Number_of_Pixels_2000	Number_of_Pixels_2019	Mean_dH_2000	Mean_dH_2019	SD_2000	SD_2019	t_stat	p_value	cohen_d
SRTMminusIGM	3224	2119	-10.895	-10.653	14.296	13.341	-0.631	0.528	-0.018
LTminusIGM	649	460	-10.607	-13.064	20.124	23.395	1.825	0.068	0.113
CBminusSRTM	764	656	-17.024	-15.285	13.824	14.452	-2.306	0.021	-0.123
CBminusIGM	764	656	-33.433	-30.247	17.248	16.093	-3.598	0.0	-0.191
LTminusSRTM	649	460	-9.077	-10.161	10.536	10.657	1.676	0.094	0.102

600 **Table F1:** Comparison of glacier elevation change statistics between 2000 and 2019 glacier inventories. Statistics include mean elevation change (mean_dH), standard deviation, t-statistic, p-value, and Cohen's d effect size.

https://doi.org/10.5194/egusphere-2025-5795
Preprint. Discussion started: 19 February 2026

References

Aguayo, R., Maussion, F., Schuster, L., Schaefer, M., Caro, A., Schmitt, P., ... & Aguayo, M. (2024, April). Unravelling the sources of uncertainty in glacier runoff in the Patagonian Andes (40-56° S). In EGU General Assembly Conference Abstracts (p. 9831).

Alvarez-Garreton, C., Mendoza, P. A., Boisier, J. P., Addor, N., Galleguillos, M., Zambrano-Bigiarini, M., Lara, A., Puelma, C., Cortes, G., Garreaud, R., McPhee, J., and Ayala, A.: The CAMELS-CL dataset: Catchment attributes and meteorology for large-sample studies – Chile dataset, Hydrol. Earth Syst. Sci., 22, 5817–5846, https://doi.org/10.5194/hess-22-5817-2018, 2018.

Ayala, Á., Farías-Barahona, D., Huss, M., Pellicciotti, F., McPhee, J., & Farinotti, D. (2020). Glacier runoff variations since 1955 in the Maipo River basin, in the semiarid Andes of central Chile. The Cryosphere, 14(6), 2005-2027.

Ayala, A., Pellicciotti, F., MacDonell, S., McPhee, J., and Burlando, P.: Modelling the hydrological response of debris-free and debris-covered glaciers to present climatic conditions in the semiarid Andes of central Chile, Hydrol. Process., 30, 4036–4058, https://doi.org/10.1002/hyp.10971, 2016.

Barria, I., Caro, A., Montecinos, A., and Leiva, C.: Simulation of long-term changes of the equilibrium line altitude in the central Chilean Andes derived from atmospheric variables during the 1958–2018 period, Front. Environ. Sci., 7, 161, https://doi.org/10.3389/fenvs.2019.00161, 2019.

Beck, H. E., Van Dijk, A. I. J. M., Levizzani, V., Schellekens, J., Miralles, D. G., Martens, B., and De Roo, A.: MSWEP: 3-hourly 0.25° global gridded precipitation (1979–2015) by merging gauge, satellite, and reanalysis data, Hydrol. Earth Syst. Sci., 21, 589–615, https://doi.org/10.5194/hess-21-589-2017, 2017.

Bellisario, A., Ferrando, F., and Janke, J.: Water resources in Chile: The critical relation between glaciers and mining for sustainable water management, Investig. Geogr., 46, 3, https://doi.org/10.5354/0719-5370.2013.30288, 2013.

Beraud, L., Cusicanqui, D., Rabatel, A., Brun, F., Vincent, C. and Six, D.: Glacier-wide seasonal and annual geodetic mass balances from Pléiades stereo images: application to the Glacier d'Argentière, French Alps, *J. Glaciol.*, 69(275), pp. 525–537, 2023. https://doi.org/10.1017/jog.2022.79

Bobadilla, A., Stehr, A., and Toro, N.: Evaluation of climate-change impacts on the temporal and spatial behaviour of drought in south-central Chile, Hydrol. Sci. J., 69, 165–184, https://doi.org/10.1080/02626667.2023.2288217, 2024.

Boisier, J. P., Rondanelli, R., Garreaud, R. D., and Muñoz, F.: Anthropogenic and natural contributions to the southeast Pacific precipitation decline and recent megadrought in central Chile, Geophys. Res. Lett., 43, 413–421, https://doi.org/10.1002/2015GL067265, 2016.

Braun, M. H., Malz, P., Sommer, C., Farías-Barahona, D., Sauter, T., Casassa, G., Soruco, A., and Seehaus, T.: Constraining glacier elevation and mass changes in South America, Nat. Clim. Change, 9, 130–136, https://doi.org/10.1038/s41558-018-0375-7, 2019.

Brock, B., Rivera, A., Casassa, G., Bown, F., & Acuña, C. (2007). The surface energy balance of an active ice-covered volcano: Villarrica Volcano, southern Chile. Annals of Glaciology, 45, 104-114.

Brüggen, J.: Contribución a la geología de los volcanes y termas de Chillán, Imprenta Universitaria, Santiago de Chile, 1948.

https://doi.org/10.5194/egusphere-2025-5795
Preprint. Discussion started: 19 February 2026

Caro, A., Vivero, S., Farías-Barahona, D., Burger, F., Seehaus, T., Schaefer, M., Rivera, A., and Braun, M. H.: Hydrological response of Andean catchments to recent glacier mass loss, The Cryosphere, 18, 2487–2507, https://doi.org/10.5194/tc-18-2487-2024, 2024.

Caro, D. A.: Estudios glaciológicos en los Nevados de Chillán, Undergraduate thesis, Univ. de Chile, Santiago, https://repositorio.uchile.cl/bitstream/handle/2250/116536/caro_d.pdf, 2014.

Carrasco-Escaff, T., Rojas, M., Garreaud, R. D., Bozkurt, D., & Schaefer, M. (2023). Climatic control of the surface mass balance of the Patagonian Icefields. The Cryosphere, 17(3), 1127-1149.

Cogley, J. G.: Geodetic and direct mass-balance measurements: Comparison and joint analysis, Ann. Glaciol., 50, 96–100, https://doi.org/10.3189/172756409787769744, 2009.

Cordero, R. R., Feron, S., Damiani, A., Carrasco, J., Karas, C., Wang, C., Kraamwinkel, C. T., and Beaulieu, A.: Extreme fire weather in Chile driven by climate change and El Niño–Southern Oscillation (ENSO), Sci. Rep., 14, 1974, https://doi.org/10.1038/s41598-023-50381-9, 2024.

Dirección General de Aguas: Inventario público de glaciares de Chile, Ministerio de Obras Públicas de Chile, Santiago, 2014.

DGA: Monitoreo de detalle del glaciar noroeste del complejo volcánico Nevados de Chillán, 2020–2021, Región de Ñuble, Ministerio de Obras Públicas, Dirección General de Aguas, Unidad de Glaciología y Nieves, Santiago, S.I.T. 519,https://repositoriodirplan.mop.gob.cl/biblioteca/server/api/core/bitstreams/b254c269-1c27-4142-a150-9ad7c30e8cf3/content, 2022.

DGA: Reporte de Balance de Masa del Glaciar Noroeste del Complejo Volcánico Nevados de Chillán, Región de Ñuble, Macrozona Sur, 2023–2024, Ministerio de Obras Públicas, Dirección General de Aguas, Unidad de Glaciología y Nieves, Santiago, S.I.T. 501, https://repositoriodirplan.mop.gob.cl/biblioteca/server/api/core/bitstreams/c865a005-3241-4213-a36d-9386b3accb96/content, 2024.

Dixon, H. J., Murphy, M. D., Sparks, R. S. J., Chávez, R., Naranjo, J. A., Dunkley, P. N., Young, S. R., Gilbert, J. S., Pringle, M. S., and Harmon, R. S.: The geology of Nevados de Chillán volcano, Chile, Rev. Geol. Chile, 26, 227–253, https://doi.org/10.4067/S0716-02081999000200006, 1999.

Dussaillant, I., Berthier, E., Brun, F., Masiokas, M., Hugonnet, R., Favier, V., Rabatel, A., Pitte, P., and Ruiz, L.: Two decades of glacier mass loss along the Andes, Nat. Geosci., 12, 802–808, https://doi.org/10.1038/s41561-019-0432-5, 2019.

Farías-Barahona, D., Vivero, S., Casassa, G., Schaefer, M., Burger, F., Seehaus, T., Iribarren-Anacona, P., Escobar, F., and Braun, M. H.: Geodetic mass balances and area changes of Echaurren Norte Glacier (Central Andes, Chile) between 1955 and 2015, Remote Sens., 11, 260, https://doi.org/10.3390/rs11030260, 2019.

Farías-Barahona, D., Ayala, Á., Bravo, C., Vivero, S., Seehaus, T., Vijay, S., ... & Braun, M. H. (2020). 60 years of glacier elevation and mass changes in the Maipo River Basin, central Andes of Chile. Remote Sensing, 12(10), 1658.

Fernandez, A.: How high is too high? Freezing level height as an essential indicator of glacier–climate regime shifts, J. Geophys. Res.-Atmos., 130, e2025JD045014, https://doi.org/10.1029/2025JD045014, 2025.

Frazier, A. and Singh, K. (Eds.): Fundamentals of capturing and processing drone imagery and data, CRC Press, Boca Raton, FL, ISBN 9780367431903, 2021.

https://doi.org/10.5194/egusphere-2025-5795
Preprint. Discussion started: 19 February 2026

Garreaud, R. D., Alvarez-Garreton, C., Barichivich, J., Boisier, J. P., Christie, D., Galleguillos, M., Le Quesne, C., McPhee, J., and Zambrano-Bigiarini, M.: The 2010–2015 megadrought in central Chile: Impacts on regional hydroclimate and vegetation, Hydrol. Earth Syst. Sci., 21, 6307–6327, https://doi.org/10.5194/hess-21-6307-2017, 2017.

Garreaud, R. D., Boisier, J. P., Alvarez-Garreton, C., Barichivich, J., Christie, D., LeQuesne, C., McPhee, J., and Zambrano-Bigiarini, M.: The Central Chile Mega Drought (2010–2018): A climate dynamics perspective, *Int. J. Climatol.*, 40, 421–439, https://doi.org/10.1002/joc.6219, 2020.

Garreaud, R. D., Alvarez-Garreton, C., Barichivich, J., Boisier, J. P., Christie, D., Galleguillos, M., LeQuesne, C., McPhee, J., and Zambrano-Bigiarini, M.: The 2010–2015 megadrought in central Chile: impacts on regional hydroclimate and vegetation, *Hydrol. Earth Syst. Sci.*, 21, 6307–6327, https://doi.org/10.5194/hess-21-6307-2017, 2017.

Farías-Barahona, D., Vivero, S., Casassa, G., Schaefer, M., Burger, F., Seehaus, T., Iribarren-Anacona, P., Escobar, F. and Braun, M. H.: Geodetic Mass Balances and Area Changes of Echaurren Norte Glacier (Central Andes, Chile) between 1955 and 2015, Remote Sens., 11(3), 260, https://doi.org/10.3390/rs11030260 , 2019.

Global Volcanism Program: Report on Nevados de Chillán (Chile) — December 2022, Smithsonian Institution, *Bull. Global Volcanism Network*, 47, https://doi.org/10.5479/si.GVP.BGVN202212-357070, 2022.

Hugonnet, R., McNabb, R., Berthier, E., Menounos, B., Nuth, C., Girod, L., Farinotti, D., Huss, M., Dussaillant, I., Brun, F., & Kääb, A.: Accelerated global glacier mass loss in the early twenty-first century, *Nature*, 592, 726–731, https://doi.org/10.1038/s41586-021-03436-z, 2021.

Huss, M.: Density assumptions for converting geodetic glacier volume change to mass change, *The Cryosphere*, 7, 877–887, https://doi.org/10.5194/tc-7-877-2013, 2013.

Huss, M. and Hock, R.: Global-scale hydrological response to future glacier mass loss, *Nat. Clim. Change*, 8, 135–140, https://doi.org/10.1038/s41558-017-0049-x, 2018.

Immerzeel, W. W., Lutz, A. F., Andrade, M., Bahl, A., Biemans, H., Bolch, T., ... & Baillie, J. E. M. (2020). Importance and vulnerability of the world's water towers. Nature, 577(7790), 364-369.

James, N. A. and Matteson, D. S.: ecp: An R Package for Nonparametric Multiple Change Point Analysis of Multivariate Data, *J. Stat. Softw.*, 62, 1–25, https://doi.org/10.18637/jss.v062.i07, 2015.

Kaufmann, V., Seier, G., Sulzer, W., Wecht, M., Liu, Q., Lauk, G., and Maurer, M.: ROCK GLACIER MONITORING USING AERIAL PHOTOGRAPHS: CONVENTIONAL VS. UAV-BASED MAPPING – A COMPARATIVE STUDY, Int. Arch. Photogramm. Remote Sens. Spatial Inf. Sci., XLII-1, 239–246, https://doi.org/10.5194/isprs-archives-XLII-1-239-2018, 2018.

Lagos-Zúñiga, M., Balmaceda-Huarte, R., Regoto, P., Torrez, L., Olmo, M., Lyra, A., Pareja-Quispe, D. and Bettolli, M. L.: Extreme indices of temperature and precipitation in South America: Trends and intercomparison of regional climate models, *Clim. Dyn.*, https://doi.org/10.1007/s00382-022-06598-2, 2022.

Lagos-Zúñiga, M., Mendoza, P. A., Campos, D., et al.: Trends in seasonal precipitation extremes and associated temperatures along continental Chile, Clim. Dyn., 62, 4205–4222, https://doi.org/10.1007/s00382-024-07127-z, 2024.

https://doi.org/10.5194/egusphere-2025-5795
Preprint. Discussion started: 19 February 2026

Li, S., Moreno, M., Bedford, J., Rosenau, M., Heidbach, O., Melnick, D., and Oncken, O.: Postseismic uplift of the Andes following the 2010 Maule earthquake: Implications for mantle rheology, Geophys. Res. Lett., 44, 1768–1776, https://doi.org/10.1002/2016GL071995, 2017.

Mark, B. G., Baraer, M., Fernandez, A., Immerzeel, W., Moore, R. D., & Weingartner, R. (2015). Glaciers as water resources. The high-mountain cryosphere: Environmental changes and human risks, 184-203.

Martínez-Retureta, R., Aguayo, M., Abreu, N. J., Stehr, A., Duran-Llacer, I., Rodríguez-López, L., Sauvage, S., and Sánchez-Pérez, J.-M.: Estimation of the climate change impact on the hydrological balance in basins of south-central Chile, Water, 13, 794, https://doi.org/10.3390/w13060794, 2021.

Matteson, D. S., and James, N. A.: A nonparametric approach for multiple change point analysis of multivariate data, J. Amer. Stat. Assoc., 109, 334–345, https://doi.org/10.1080/01621459.2013.849605, 2014.

McCarthy, M., Meier, F., Fatichi, S., Stocker, B. D., Shaw, T. E., Miles, E., Dussaillant, I., and Pellicciotti, F.: Glacier contributions to river discharge during the current Chilean megadrought, Earth's Future, 10, e2022EF002852, https://doi.org/10.1029/2022EF002852, 2022.

Mejías, A., McPhee, J., Mahmoud, H., Farías-Barahona, D., Kinnard, C., MacDonell, S., Montserrat, S., Somos-Valenzuela, M., and Fernandez, A.: Multidecadal estimation of hydrological contribution and glacier mass balance in the semi-arid Andes based on physically based modeling and geodetic mass balance, Front. Earth Sci., 13, 1517081, https://doi.org/10.3389/feart.2025.1517081, 2025.

Mendoza, P. A., Musselman, K. N., Revuelto, J., Deems, J. S., López-Moreno, J. I., and McPhee, J.: Interannual and seasonal variability of snow depth scaling behavior in a subalpine catchment, Water Resour. Res., 56, e2020WR027343, https://doi.org/10.1029/2020WR027343 , 2020.

Naranjo, J.A., Gilbert, J., & Sparks, R.S.J.: Geología del Complejo Volcánico Nevados de Chillán, Región del Biobío, Gobierno de Chile: Servicio Nacional de Geología y Minería, 2008.

Novoa Lizama, C., Remy, D., Baez, J. C., Oyarzun, A., Bonvalot, S., and Hooper, A.: Modeling magma recharge dynamics during the 2016 Nevados de Chillán eruption: An interacting two-chamber system evidenced by petrology and geodesy, J. Volcanol. Geotherm. Res., 458, 108253, https://doi.org/10.1016/j.jvolgeores.2024.108253 , 2025.

Nuth, C., & Kääb, A.: Co-registration and bias corrections of satellite elevation data sets for quantifying glacier thickness change, *Cryosphere*, 5, 271–290, https://doi.org/10.5194/tc-5-271-2011, 2011.

Owen, L.A., Thackray, G., Anderson, R.S., Briner, J., Kaufman, D., Roe, G., Pfeffer, W., & Yi, C.: Integrated research on mountain glaciers: current status, priorities and future prospects, *Geomorphology*, 103, 158–171, 2009.

Philippi, R.: Exkursion nach den Bädern und dem Neuen Vulkan von Chillan in Chile, im Spätsommer 1862 gemacht, *Petermanns Geogr. Mitt.*, 1863, 241–257.

Poveda, G., Espinoza, J. C., Zuluaga, M. D., Solman, S. A., Garreaud, R., and van Oevelen, P. J.: High impact weather events in the Andes, Front. Earth Sci., 8, 162, https://doi.org/10.3389/feart.2020.00162, 2020.

https://doi.org/10.5194/egusphere-2025-5795
Preprint. Discussion started: 19 February 2026

Rabatel, A., Sirguey, P., Drolon, V., Maisongrande, P., Arnaud, Y., Berthier, E., Davaze, L., Dedieu, J.-P., and Dumont, M.: Annual and seasonal glacier-wide surface mass balance quantified from changes in glacier surface state: a review on existing methods using optical satellite imagery, Remote Sens., 9, 507, https://doi.org/10.3390/rs9050507, 2017.

Ragettli, S., & Pellicciotti, F.: Calibration of a physically based, spatially distributed hydrological model in a glacierized basin: On the use of knowledge from glaciometeorological processes to constrain model parameters, *Water Resour. Res.*, 48, 2011WR010559, https://doi.org/10.1029/2011WR010559, 2012.

RGI Consortium: Randolph Glacier Inventory – A dataset of global glacier outlines, Version 6, *Natl. Snow Ice Data Cent.*, https://doi.org/10.7265/4M1F-GD79, 2017.

Rivera, A., Bown, F., Mella, R., Wendt, J., Casassa, G., Acuña, C., Rignot, E., Clavero, J., and Brock, B.: Ice volumetric changes on active volcanoes in southern Chile, Ann. Glaciol., 43, 111–122, https://doi.org/10.3189/172756406781811970, 2006.

Rossini, M., Garzonio, R., Panigada, C., Tagliabue, G., Bramati, G., Vezzoli, G., Cogliati, S., Colombo, R., and Di Mauro, B.: Mapping Surface Features of an Alpine Glacier through Multispectral and Thermal Drone Surveys, Remote Sens., 15, 3429, https://doi.org/10.3390/rs15133429, 2023.

Rounce, D. R., Hock, R., McNabb, R. W., Millan, R., Sommer, C., Braun, M. H., Malz, P., Maussion, F., Mouginot, J., Seehaus, T. C., and Shean, D. E.: Distributed Global Debris Thickness Estimates Reveal Debris Significantly Impacts Glacier Mass Balance, Geophys. Res. Lett., 48, e2020GL091311, https://doi.org/10.1029/2020GL091311, 2021.

Rubio-Álvarez, E., & McPhee, J.: Patterns of spatial and temporal variability in streamflow records in south central Chile in the period 1952–2003, *Water Resour. Res.*, 46, https://doi.org/10.1029/2009WR007982, 2010.

Schaefer, M., Machguth, H., Falvey, M., Casassa, G., & Rignot, E. (2015). Quantifying mass balance processes on the Southern Patagonia Icefield. The Cryosphere, 9(1), 25-35.

Schumacher, V., Justino, F., Fernández, A., Meseguer Ruiz, O., Sarricolea, P., Comin, A., Peroni Venancio, L., & Althoff, D.: Comparison between observations and gridded data sets over complex terrain in the Chilean Andes: Precipitation and temperature, 2020.

Schuster, L., Rounce, D.R., & Maussion, F.: Glacier projections sensitivity to temperature-index model choices and calibration strategies, *Ann. Glaciol.*, 64, 293–308, 2023.

Sen, P.K.: Estimates of the regression coefficient based on Kendall's tau, *J. Am. Stat. Assoc.*, 63, 1379–1389, 1968.

Servicio Nacional de Geología y Minería: Complejo Volcánico Nevados de Chillán, Red Nacional de Vigilancia Volcánica, https://rnvv.sernageomin.cl/complejo-volcanico-nevados-de-chillan/, 2025.

Shean, D. E., Alexandrov, O., Moratto, Z. M., Smith, B. E., Joughin, I. R., Porter, C., and Morin, P.: An automated, open-source pipeline for mass production of digital elevation models (DEMs) from very-high-resolution commercial stereo satellite imagery, ISPRS J. Photogramm. Remote Sens., 116, 101–117, https://doi.org/10.1016/j.isprsjprs.2016.03.012, 2016.

Ultee, L., Coats, S., & Mackay, J. (2022). Glacial runoff buffers droughts through the 21st century. Earth System Dynamics, 13(2), 935-959.

https://doi.org/10.5194/egusphere-2025-5795
Preprint. Discussion started: 19 February 2026

USGS EROS Archive: Digital Elevation – Shuttle Radar Topography Mission (SRTM) 1 Arc-Second Global, *U.S. Geol. Surv.*, 2018, https://www.usgs.gov/centers/eros/science/usgs-eros-archive-digital-elevation-shuttle-radar-topography-mission-srtm-1.

Centro de Estudios Científicos: Variaciones recientes de glaciares en Chile, según principales zonas glaciológicas, *Dirección General de Aguas*, 2011, https://glaciologia.cl/wp-content/uploads/2020/08/InformeVariacionesGlaciaresdga2011.pdf.

Webb, M. J., Winter, J. M., Spera, S. A., Chipman, J. W., and Osterberg, E. C.: Water, agriculture, and climate dynamics in central Chile's Aconcagua River Basin, Phys. Geogr., 42, 395–415, https://doi.org/10.1080/02723646.2020.1790719, 2020.

Westoby, M. J., Brasington, J., Glasser, N. F., Hambrey, M. J., and Reynolds, J. M.: 'Structure-from-Motion' photogrammetry: A low-cost, effective tool for geoscience applications, Geomorphology, 179, 300–314, https://doi.org/10.1016/j.geomorph.2012.08.021, 2012.

Wigmore, O., & Mark, B.: Monitoring tropical debris-covered glacier dynamics from high-resolution unmanned aerial vehicle photogrammetry, Cordillera Blanca, Peru, *Cryosphere*, 11, 2463–2480, https://doi.org/10.5194/tc-11-2463-2017, 2017.

Wigmore, O., & Molotch, N.P.: Weekly high-resolution multi-spectral and thermal uncrewed-aerial-system mapping of an alpine catchment during summer snowmelt, Niwot Ridge, Colorado, *Earth Syst. Sci. Data*, 15, 1733–1747, https://doi.org/10.5194/essd-15-1733-2023, 2023.

Zemp, M., Frey, H., Gärtner-Roer, I., Nussbaumer, S. U., Hoelzle, M., Paul, F., ... & Vincent, C. (2015). Historically unprecedented global glacier decline in the early 21st century. Journal of glaciology, 61(228), 745-762.

Zenteno, P.: Variaciones recientes de los glaciares en la zona centro sur de Chile y su relación con los cambios climáticos y la actividad volcánica, Undergraduate thesis, Universidad de Chile, Facultad de Arquitectura y Urbanismo, 2008.